Article

Synthesis and Biological Evaluation of Substituted Fused Dipyranoquinolinones

Evangelia-Eirini N. Vlachou [1] , **Eleni Pontiki** [2] , **Dimitra J. Hadjipavlou-Litina** [2,*] and **Konstantinos E. Litinas** [1,*]

1   Laboratory of Organic Chemistry, Department of Chemistry, Aristotle University of Thessaloniki, 54124 Thessaloniki, Greece; e.e.vlachou@gmail.com

2   Department of Pharmaceutical Chemistry, School of Pharmacy, Faculty of Health Sciences, Aristotle University of Thessaloniki, 54124 Thessaloniki, Greece; epontiki@pharm.auth.gr

*   Correspondence: hadjipav@pharm.auth.gr (D.J.H.-L.); klitinas@chem.auth.gr (K.E.L.)

Abstract: New methyl-substituted, and diphenyl-substituted fused dipyranoquinolinones are prepared in excellent yields via the triple bond activation and *6-endo-dig* cyclization of propargyloxy-coumarin derivatives by gold nanoparticles supported on TiO_2 in chlorobenzene under microwave irradiation. In the absence of gold nanoparticles, the methyl-substituted propargyloxycoumarin derivatives resulted in fused furopyranoquinolinones through Claisen rearrangement and *5-exo-dig* cyclization. The intermediate propargyloxy-fused pyridocoumarins are prepared by propargylation of the corresponding hydroxy-fused pyridocoumarins. The methyl-substituted derivatives of the latter are synthesized in excellent yield by the three-component reaction of amino hydroxycoumarin with *n*-butyl vinyl ether under iodine catalysis. The diphenyl-substituted derivatives of hydroxy-fused pyridocoumarins are obtained, also, by the three-component reaction of amino hydroxycoumarin with benzaldehyde and phenyl acetylene catalyzed by iron (III) chloride. Preliminary biological tests of the title compounds indicated lipoxygenase (LOX) (EC 1.13.11.12) inhibitory activity (60–100 μM), whereas compound **28a**, with $IC_{50} = 10$ μM, was found to be a potent LOX inhibitor and a possible lead compound. Only compounds **10b** and **28b** significantly inhibited lipid peroxidation.

Keywords: fused dipyranoquinolinones; fused pyridocoumarins; iodine catalysis; *n*-butyl vinyl ether; Au-nanoparticles; fused furopyranoquinolinones; multi-component reactions; Fe (III) trichloride catalysis; lipoxygenase inhibition

1. Introduction

The coumarin moiety is present in many natural products and in synthetic bioactive compounds [1–9]. Coumarin derivatives are recognized for their biological properties, such as anticancer, anti-inflammatory, antioxidant, antitubercular, anti-*Helicobacter pylori*, anti-Alzheimer's, antifungal, and anticoagulant [10–19]. Many fused coumarin derivatives containing pyridine or pyran moieties can also be isolated from natural sources and have shown interesting biological activities; santiagonamine (**I**) (Figure 1) has been isolated from the extracts of *Berberis darwinii* Hook presenting wound-healing activity [20,21]; ganocochliarine F (**II**) can be extracted from *Ganoderma cochlear* and has been evaluated for renal fibrosis [22]; goniothaline A (**III**) and goniothaline B (**IV**) have been isolated from *Goniothalamus Australis*, an Australian rainforest plant, and evaluated for in vitro antimalarial activity [23,24], and likewise, polynemoraline C (**V**) has been isolated from the ethanol extracts of the branches and leaves of *Polyalthia nemoralis* A DC [25], and found to exhibit anticholinergic, anti-inflammatory, antitumor, and antimicrobial activities [26].

Similarly, the fused pyranocoumarins seselin (**VI**) and xanthyletin (**VII**) can be isolated from the citrus roots of plants of the *Rutaceae* family and from the root bark of *Paramignya monophyla*, respectively, and have been found to present moderate DNA damage and

evaluated for in vitro cytotoxicity in L1210 murine leukemia [27,28]. **VI** was also found to inhibit multiple SARS-CoV-2 proteins [29], while **VII** was found to exert antifungal activity [30]. Another example is decursinol (**VIII**) isolated from the Korean medicinal herb *Angelica gigas* Nakai that exhibits inhibitory activity toward AChE in vitro [31].
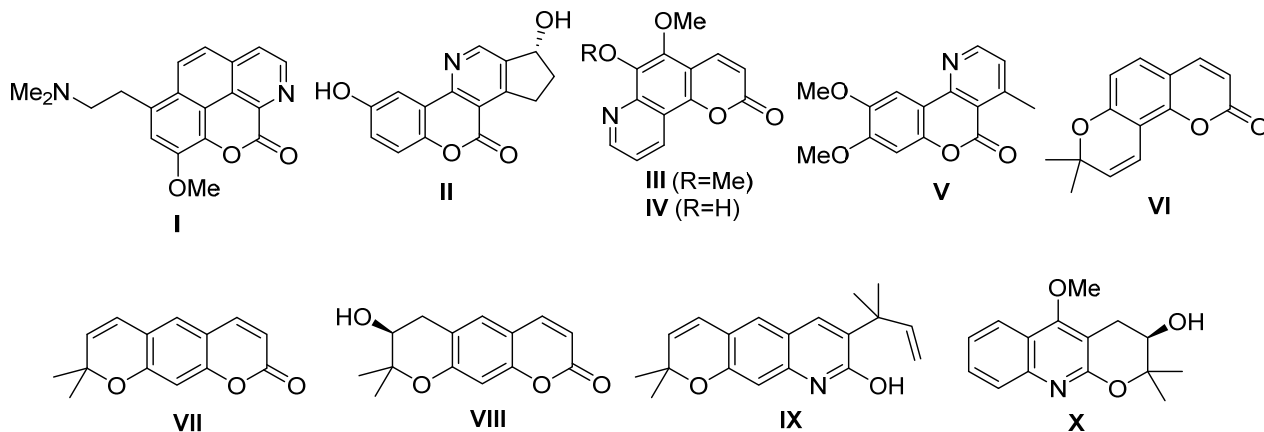

Figure 1. Natural biologically active fused pyridocoumarins, pyranocoumarins, and pyranoquinolines.

Fused pyranoquinoline derivatives are, also, present in nature, such as helietidine (**IX**) and (-)-(*R*)-geibalansin (**X**). The former, helietidine, can be isolated from the stem bark and the leaves of *Helietta longifoliata* Britt (Rutaceae family) and has been found to present antibacterial activity [32]. The latter, (-)-(*R*)-geibalansin, can be found as a metabolite from *Zanthoxylum hyemale* (Rutaceae) and can be prepared in an asymmetric total synthesis from 5-methoxy-2,2-dimethyl-(2*H*)pyrano[2,3-*b*]quinoline [33]. Finally, racemic geibalansin, also isolated from the stem bark of *Citrus maxima* (Burm). Merr. (Rutaceae), possesses significant bioactivity [34].

A lot of methods have been used for the synthesis of pyridocoumarins, starting mainly from aminocoumarins. Skraup, Skraup–Doebner–von Miller, Povarov, Friedlander, multi-component (MCR), and metal-catalyzed reactions are among the most familiar reactions for the synthesis of fused pyridocoumarins [35,36]. The formation of the pyran moiety of fused pyranocoumarins is achieved mainly by the Claisen rearrangement of propargyloxycoumarins followed by cyclization [37] or by the reaction of hydroxycoumarins with α,β-unsaturated aldehydes or ketones [38]. In this paper, we build on our extensive experience in the synthesis of fused pyridocoumarin [39–46] and pyranocoumarin derivatives [47–52], and recently published work on fused coumarins with pyridine and pyran moieties [39], and propose the synthesis and biological evaluation of substituted fused pyridopyranocoumarins. We are using new substituted fused pyridocoumarins, which, through the propargyloxy derivatives, are transformed to the title compounds via Au-nanoparticles catalysis. The reactions studied and the products prepared are depicted in Schemes 1–3.
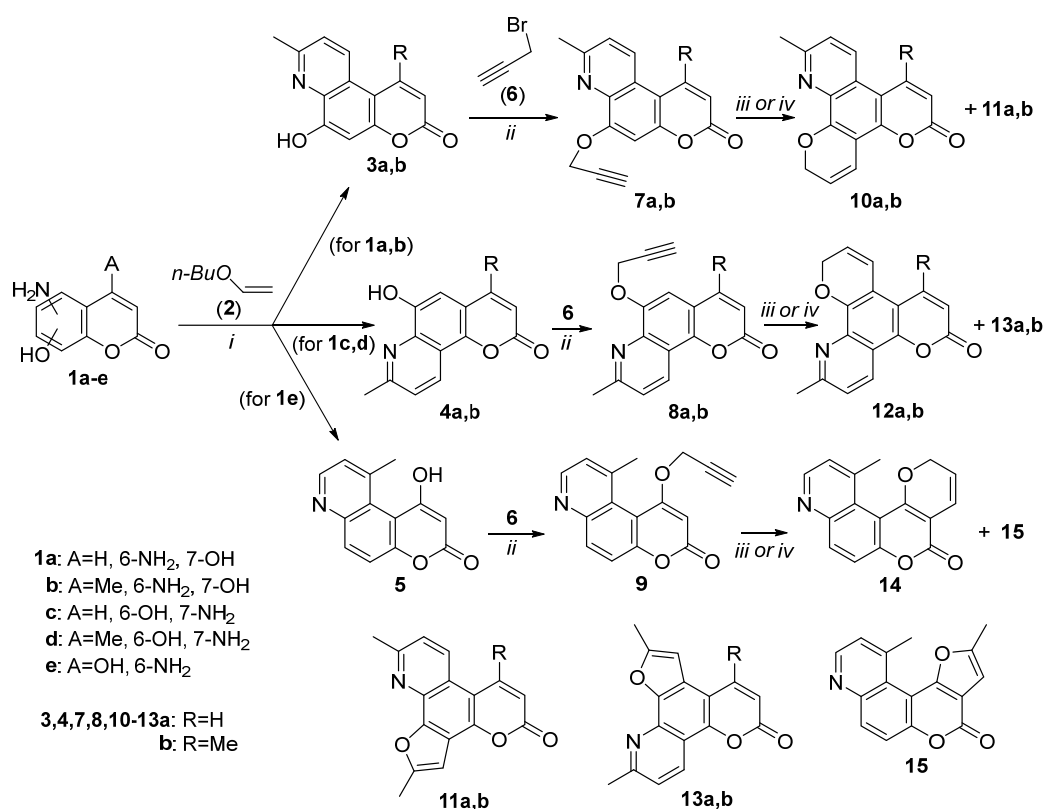
Scheme 1. *Reagents and conditions: (i)* **2** (3 equiv.), I$_2$ (10 mol%), CH$_3$CN, reflux, 1 h; *(ii)* **6** (1.1 equiv.), Cs$_2$CO$_3$ (1.1 equiv.), acetone, MW, 100 °C, 10 min; *(iii)* Au/TiO$_2$ (4 mol%), PhCl, MW, 180 °C, 2 h (for **10a**, **b**, **12a**, **b**, **14**); *(iv)* PhCl, MW, 180 °C, 2.5 h (for **11a,b**, **13a,b**, **15**).
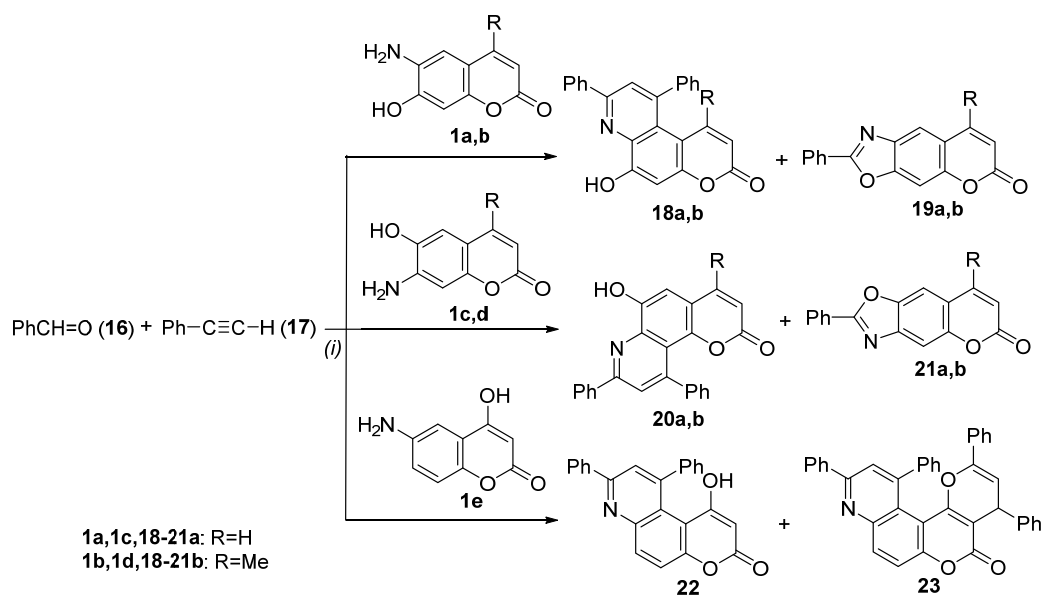
Scheme 2. *Reagents and conditions: (i)* **16** (1.1 equiv.), **17** (1.1 equiv.), FeCl$_3$·H$_2$O (10 mol%), toluene, reflux, 24 h.
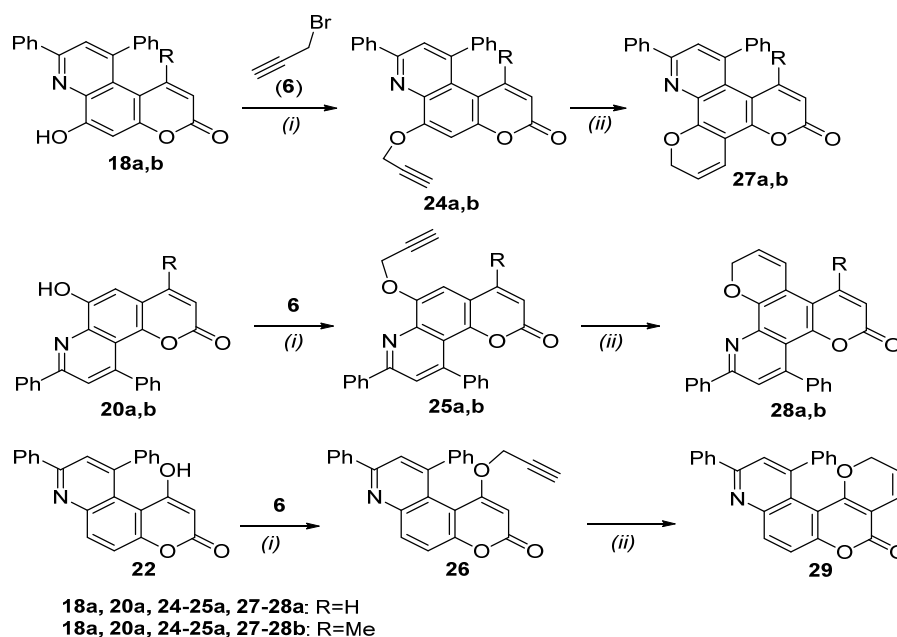
Scheme 3. *Reagents and conditions: (i)* **6** (1.1 equiv.), Cs$_2$CO$_3$ (1.1 equiv.), acetone, MW, 100 °C, 5 min; *(ii)* Au/TiO$_2$ (4 mol%), PhCl, MW, 180 °C, 2 h.

2. Results and Discussion

2.1. Chemistry

The reactions for the synthesis of the methyl-substituted pyridine moiety of fused pyridocoumarins are presented in Scheme 1. The starting compounds, hydroxyaminocoumarins **1a,b** [53,54] and **1c–e** [39,55,56] were prepared by the Pd-catalyzed reduction of the corresponding hydroxynitrocoumarins in methanol under an H$_2$ atmosphere at room temperature [39]. The reaction of 6-amino-7-hydroxycoumarin (**1a**) with an excess of *n*-butyl vinyl ether (**2**) in the presence of a catalytic amount (10%) of I$_2$ in CH$_3$CN under reflux for 1 h resulted in the preparation of 6-hydroxy-8-methyl-3*H*-pyrano[3,2-*f*]quinolin-3-one (**3a**) (see Supplementary Materials) in a 94% yield (Scheme 1, Table 1, entry 1). This is an application of the former three-component, Povarov-type, reaction for the synthesis of fused pyridocoumarins [41]. The structure of **3a** is revealed from the ^{1}H-NMR spectrum, where the 9-H and 10-H of the pyridine moiety appears at 7.50 (d, *J* = 8.6 Hz) and 8.36 (d, *J* = 8.6 Hz) ppm, respectively, and the NOESY-1D experiment, where the 1-H at 8.21 (*J* = 9.6 Hz) ppm of the coumarin moiety is correlated with 8.36 (10-H) (8.6%) and 6.37 (*J* = 9.6 Hz, (2-H) (3.2%).

The similar reaction of 6-amino-7-hydroxy-4-methylcoumarin (**1b**) with **2** in the presence of I$_2$ (10 mol%) gave the 4-methyl-substituted derivative **3b** in an 86% yield (Table 1, entry 2). The NOESY-1D experiments showed a correlation of the 1-CH$_3$ protons at 2.83 ppm with 10-H at 8.80 ppm (2.25%) and 2-H at 6.20 ppm (1%), revealing the same regioselectivity as compound **3a**. The analogous reactions of 7-amino-6-hydroxycoumarin (**1c**) and 7-amino-6-hydroxy-4-methylcoumarin (**1d**) with an excess of *n*-butyl vinyl ether (**2**) led to the [7,8]-fused pyridocoumarins **4a** and **4b** in 98% and 87% yields, respectively (Table 1, entries 3,4). The reaction of 6-amino-4-hydroxycoumarin (**1e**) with **2** in the presence of I$_2$ (10 mol%) resulted in the [5,6]-fused pyridocoumarin **5** in a 90% yield (Table 1, entry 5), with different regioselectivity in the three-component reaction. The downfield proton at 9.38 ppm is the 8-H near the nitrogen of the pyridine moiety as indicated by the correlation with the 9-H at 7.41 ppm (2.6%), which is correlated also (0.6%) with 10-CH$_3$ protons at 2.76 ppm.

Table 1. Synthesis of hydroxy-fused pyridocoumarins **3a,b**, **4a,b**, **5**, propargyloxy-fused pyrido-coumarins **7a,b**, **8a,b**, **9**, fused dipyranoquinolinones **10a,b**, **12a,b**, **14**, and fused furopyranoquinoli-nones **11a,b**, **13a,b**, **15**.

Entry	Reacting Compounds	Reaction Conditions	Product (Yield, %)
1	**1a, 2** (3 equiv.)	**A**: I_2 (10 mol%), CH_3CN, reflux, 1 h	**3a** (94)
2	**1b, 2** (3 equiv.)	**A**	**3b** (86)
3	**1c, 2** (3 equiv.)	**A**	**4a** (98)
4	**1d, 2** (3 equiv.)	**A**	**4b** (87)
5	**1e, 2** (3 equiv.)	**A**	**5** (90)
6	**3a, 6** (1.1 equiv.)	**B**: Cs_2CO_3 (1.1 equiv.), acetone, MW, 100 °C, 10 min	**7a** (99)
7	**3b, 6** (1.1 equiv.)	**B**	**7b** (93)
8	**4a, 6** (1.1 equiv.)	**B**	**8a** (97)
9	**4b, 6** (1.1 equiv.)	**B**	**8b** (93)
10	**5, 6** (1.1 equiv.)	**B**	**9** (99)
11	**7a**	**C**: Au/TiO_2 (4 mol%), PhCl, MW, 180 °C, 2 h	**10a** (96)
12	**7b**	**C**	**10b** (93)
13	**8a**	**C**	**12a** (96)
14	**8b**	**C**	**12b** (91)
15	**9**	**C**	**14** (94)
16	**7a**	**D**: PhCl, MW, 180 °C, 2.5 h	**11a** (90)
17	**7b**	**D**	**11b** (98)
18	**8a**	**D**	**13a** (95)
19	**8b**	**D**	**13b** (93)
20	**9**	**D**	**15** (93)

The mechanism of the above-mentioned reactions for the synthesis of compounds **3a,b** and **4a,b** is similar to that proposed by us previously [41,46]. In the case of the 6-amino-4-hydroxycoumarin (**1e**), the *o*-position to the amine was added to the vinyl ether located near the hydroxyl group through iodine catalysis to form intermediate **A** (Scheme 4). Elimination of *n*-butanol led to **B,** and then a 1,3-H shift led to the imine **C**. The Aza-Diels–Alder reaction of the latter with a second molecule of vinyl ether **2** gave adduct **D**, which, upon elimination of *n*-butanol to intermediate **E** and air oxidation, resulted in the final product **5**.

Propargylation of the new hydroxy derivatives of fused pyridocoumarins **3a,b**, **4a,b**, **5** with propargyl bromide (**6**) in the presence of Cs_2CO_3 under microwave irradiation led to the corresponding derivatives **7a,b**, **8a,b**, **9** in excellent yields (Table 1, entries 6–10). With the propargyloxy derivatives of fused pyridocoumarins in hand (Scheme 1), the optimal conditions for their cyclization to the corresponding pyran derivatives were investigated using 1,8-dimethyl-6-(prop-2-yn-1-yloxy)-3*H*-pyrano[3,2-*f*]quinolin-3-one (**7b**) as the model substrate (Table 2). At first, we attempted the cyclization of **7b** in the presence of Au/TiO_2 (4 mol%) in DCE under microwave irradiation at 140 °C according to the recently reported synthesis of fused pyranocoumarins [39,47]. The starting compound remained unchanged (Table 2, entry 1). Next, no reaction was observed during the heating of **7b** in the presence of $BF_3 \cdot Et_2O$ in DMF under microwaves at 200 °C or of $AgNO_3$ (10 mol%) in DCE under MW irradiation at 140 °C, in analogy to the literature [47,57] (Table 2, entries 2,3). Compound **7b** was cyclized to 8,11-dimethyl-2*H*,6*H*-dipyrano[3,2-*f*:3',2'-*h*]quinolin-6-one (**10b**) in a 93% yield by increasing the temperature to 180 °C in a MW oven with PhCl as the solvent [31] in the presence of Au/TiO_2 (4 mol%) (Table 2, entry 4). The presence of the pyran ring in **10b** is evident from the ^{1}H-NMR spectrum, where the 2-H, 3-H, and 4-H of the pyran moiety appeared at 5.24 (dd, J_1 = 2.0 Hz, J_2 = 3.5 Hz, 2H), 5.98 (dt, J_1 = 3.5 Hz, J_2 = 10.1 Hz, 1H), and 7.12 (d, J = 10.1 Hz, 1H) ppm, respectively. The protons of the propargyloxy group of compound **7b** at 2.60 (t, J = 2.3 Hz, 1H), and 5.07 (d, J = 2.3 Hz, 2H) ppm, and 5-H at 7.27 (s, 1H) ppm have disappeared.
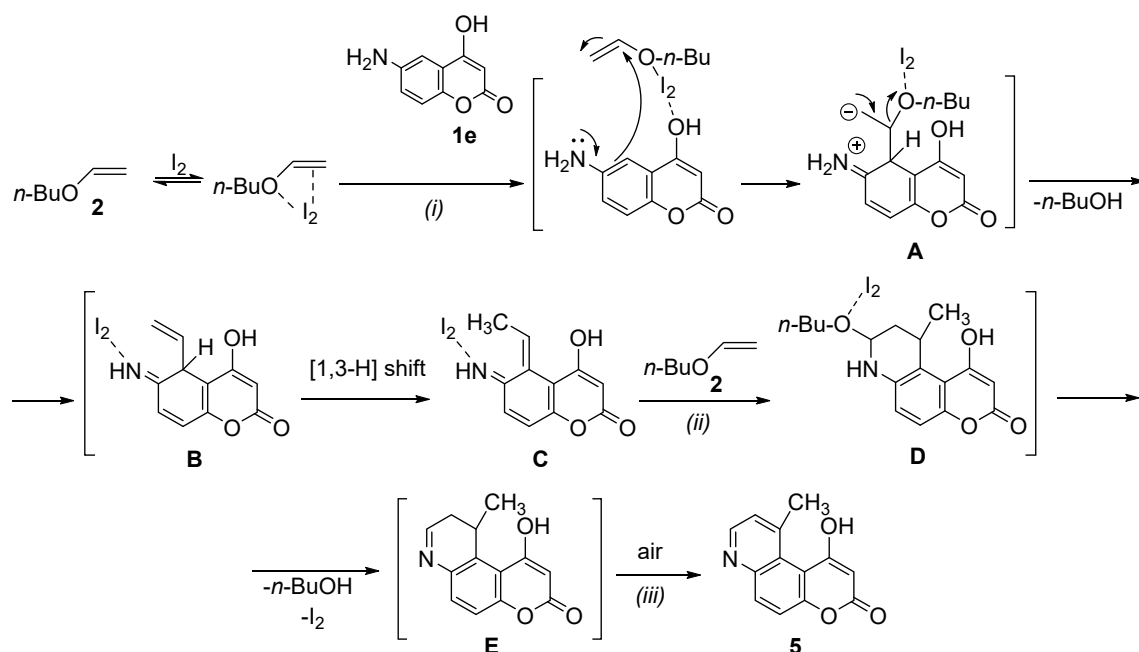
Scheme 4. *(i)* Lewis acid imine formation. *(ii)* Aza-Diels–Alder reaction catalyzed by Lewis acid, followed by elimination of n-butanol. *(iii)* Oxidation.

Table 2. Optimization of the conditions for the cyclization of 1,8-dimethyl-6-(prop-2-yn-1-yloxy)-3*H*-pyrano[3,2-*f*]quinolin-3-one (**7b**).

Entry	Conditions	Products (Yield %)
1	Au/TiO$_2$ (4 mol%), DCE, MW, 140 °C, 3 h	-
2	BF$_3$·Et$_2$O, DMF, MW, 200 °C, 1 h	-
3	AgNO$_3$ (10 mol%), DCE, MW, 140 °C, 1 h	-
4	Au/TiO$_2$ (4 mol%), PhCl, MW, 180 °C, 2 h	**10b** (93)
5	TiO$_2$ (4 mol%), PhCl, MW, 180 °C, 3 h	**11b** (99)
6	PhCl, MW, 180 °C, 2.5 h	**11b** (98)
7	PhCl, 120 °C, 24 h	**11b** (10), **7b** (90)
8	AuCl$_3$ (4 mol%), PhCl, MW, 180 °C, 30 min	**10b** (90)
9	AuCl (4 mol%), PhCl, MW, 180 °C, 1 h	**10b** (50), **11b** (50)

The effectiveness of Au-NPs was checked when the above reaction was performed with TiO$_2$ in PhCl at 180 °C and resulted in the formation of 2,7,10-trimethyl-5*H*-furo[3,2-*h*]pyrano[3,2-*f*]quinolin-5-one (**11b**) in a 99% yield (Table 2, entry 5). In the absence of TiO$_2$, the furan derivative **11b** was prepared also in very high yield (98%) (Table 2, entry 6). The heating in PhCl at 120 °C of **7b** for 24 h without MW irradiation led only to 10% of **11b**, while 90% of **7b** was recovered (Table 2, entry 7). We have tried also the catalysis with AuCl$_3$ or AuCl, as the Au(III) and Au(I) species are presumably responsible for the catalytic activity of Au/TiO$_2$ [42,58]. In the case of AuCl$_3$, only **10b** was isolated, in a 90% yield, while with AuCl both **10b** and **11b** were obtained (Table 2, entries 8,9). In the ^{1}H-NMR spectrum of compound **11b**, there are three CH$_3$ group at 2.66 (s, 3H), 2.84 (s, 3H), 2.91 (s, 3H) ppm and 3-H at 6.90 (s, 1H) ppm.

It seems from the above investigation that the pyran ring is formed during the catalyzed cycloisomerization of **7b** in the presence of Au/TiO$_2$, while the furan ring is prepared under the heating at high temperature in PhCl without a catalyst. Following these observations, treatment of propargyloxy derivatives **7a,b**, **8a,b**, and **9** with Au/TiO$_2$ in PhCl under MW irradiation at 180 °C for 2 h resulted in the regioselective preparation of fused pyran derivatives **10a,b**, **12a,b**, and **14**, respectively (Scheme 1), as the sole products in excellent yields (Table 1, entries 11–15). The same starting compounds under MW irradiation without

a catalyst in PhCl at 180 °C for 2.5 h led regioselectively to the fused furan derivatives **11a**,**b**, **13a**,**b**, **15**, respectively, as the sole products in excellent yields (Table 1, entries 16–20).

The regioselectivity of 6-*endo-dig* transformation of the above propargyl derivatives under treatment with Au/TiO$_2$ in a MW oven to the synthesis of the corresponding six-membered derivatives is consistent with the catalysis with Au(III) and Au(I) salts [58–62]. The regioselectivity of 5-*exo-dig* transformation of the propargyl derivatives in PhCl under MW irradiation at 180 °C to the synthesis of five-membered derivatives has been observed during the heating under force conditions (>200 °C, in diethylaniline) [63]. These regioselective reactions follow possibly the mechanistic scenarios presented in Scheme 5. Electrophilic aromatic substitution of the activated alkyne-Au-π complex **A** by the arene, following the Friedel–Crafts hydroarylation of alkynes [58,62,64,65], resulted in the vinyl-Au intermediate **B** *via* a 6-*endo-dig* cyclization. A 1,3-H shift led to the fused pyran derivative **10b** under re-generation of the catalyst. The synthesis of the furan derivative **11b** in the presence of AuCl (Table 2, entry 9) could be assumed by the transformation of the Au-intermediate **B** to the Au-salt **C** followed by a 1,3-H shift to form the *o*-allenyl naphthol derivative **D**. The 5-*exo-dig* cyclization of the latter gave the fused furan derivative **11b**. The preparation of **11b** through the heating in PhCl under MW irradiation could be explained by the Claisen rearrangement of **7b** to allenyl ketone **E**, followed by tautomerization to *o*-allenyl phenol **D** and 5-*exo-dig* cyclization.
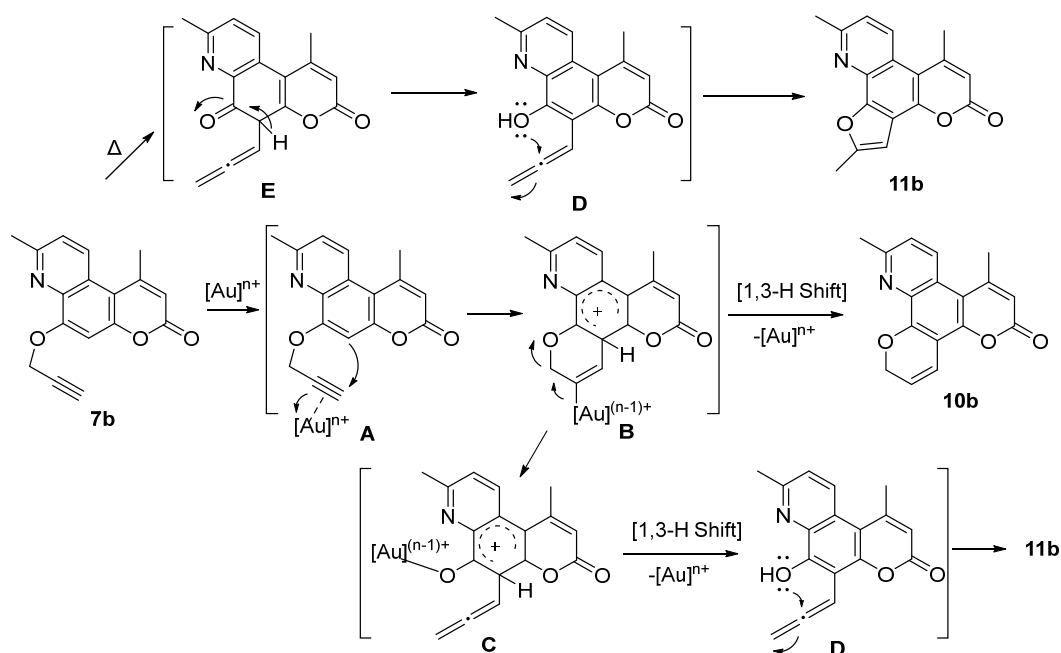
Scheme 5. Possible mechanistic pathways for the transformations of propargyloxy derivatives to fused pyran or furan derivatives.

We studied next the synthesis of fused pyridocoumarins with a diphenyl-substituted pyridine moiety (Schemes 2 and 3). The three-component reaction of 6-amino-7-hydroxycoumarin (**1a**) with benzaldehyde (**16**) and phenylacetylene (**17**) in the presence of FeCl$_3$·6H$_2$O (10 mol%) in toluene under reflux for 24 h, according to our previous synthesis of diphenyl-substituted fused pyridocoumarins [40], resulted in the synthesis of 6-hydroxy-8,10-diphenyl-3*H*-pyrano[3,2-*f*]quinolin-3-one (**18a**) and 2-phenyl-6*H*-chromeno[6,7-*d*]oxazol-6-one (**19a**) in 66% and 32% yields, respectively (Table 3, entry 1). In the ^{1}H-NMR spectrum of **18a** the 1-H, 2-H, 5-H, and 9-H of pyranone, benzo, and pyridine moieties appeared at 7.18 (d, *J* = 10.0 Hz, 1H), 5.88 (d, *J* = 10.0 Hz, 1H), 7.20 (s, 1H), and 7.90 (s, 1H), respectively, along with the 10 protons of the phenyl rings. Oxazolocoumarin **19a** is known from the literature [66]. The analogous reaction of 6-amino-7-hydroxy-4-methylcoumarin (**1b**) with

16 and **17** in the presence of FeCl$_3$·6H$_2$O (10 mol%) led to the pyridocoumarin **18b** and oxazolocoumarin **19b** (Table 3, entry 2).

Table 3. Synthesis of hydroxy-fused pyridocoumarins **18a,b**, **20a,b**, **22**, propargyloxy-fused pyrido-coumarins **24a,b**, **25a,b**, **26**, and fused dipyranoquinolinones **27a,b**, **28a,b**, **29**.

Entry	Reacting Compounds	Reaction Conditions	Products (Yield, %)
1	**1a**, **16** (1.1 equiv.), **17** (1.1 equiv.)	**E:** FeCl$_3$·6H$_2$O (10 mol%), toluene, reflux, 24 h	**18a** (66), **19a** (32)
2	**1b**, **16** (1.1 equiv.), **17** (1.1 equiv.)	E	**18b** (62), **19b** (35)
3	**1c**, **16** (1.1 equiv.), **17** (1.1 equiv.)	E	**20a** (65), **21a** (29)
4	**1d**, **16** (1.1 equiv.), **17** (1.1 equiv.)	E	**20b** (63), **21b** (33)
5	**1e**, **16** (1.1 equiv.), **17** (1.1 equiv.)	E	**22** (82), **23** (10)
6	**18a**, **6** (1.1 equiv.)	**F:** Cs$_2$CO$_3$ (1.1 equiv.), acetone, MW, 100 °C, 5 min	**24a** (99)
7	**18b**, **6** (1.1 equiv.)	F	**24b** (92)
8	**20a**, **6** (1.1 equiv.)	F	**25a** (98)
9	**20b**, **6** (1.1 equiv.)	F	**25b** (95)
10	**22**, **6** (1.1 equiv.)	F	**26** (98)
11	**24a**	**C:** Au/TiO$_2$ (4 mol%), PhCl, MW, 180 °C, 2 h	**27a** (97)
12	**24b**	C	**27b** (99)
13	**25a**	C	**28a** (96)
14	**25b**	C	**28b** (93)
15	**26**	C	**29** (92)

The three-component reactions of 7-amino-6-hydroxycoumarins **1c,d** with **16** and **17** catalyzed by FeCl$_3$·H$_2$O gave pyridocoumarins **20a,b** and oxazolocoumarins **21a,b** (Table 3, entries 3,4). From the similar reaction of 6-amino-4-hydroxycoumarin (**1e**) with **16** and **17** the angular pyridocoumarin **22** was obtained in an 82% yield, while the 2,4,10,12-tetraphenyl-4*H*,5*H*-pyrano[2′,3′:4,5]pyrano[3,2-*f*]quinolin-5-one (**23**) (10%) was also isolated (Table 3, entry 5). Compound **23** is a new product, presenting in the ^{1}H-NMR spectrum two doublets at 5.85 (*J* = 4.9 Hz) and 4.72 (*J* = 4.9 Hz) for the 3-H and 4-H, quite analogous to the protons of 2,4-diphenylpyrano[3,2-*c*]chromen-5(4*H*)-one [67]. The also expected [40] linear isomer of **22** was not detected in the reaction mixture. The reason for this was presumably the complexation of FeCl$_3$ with the triple bond and 4-OH group in the intermediate **C** formed by the reaction of imine **A** with iron (III) acetylide **B** (Scheme 6). Intramolecular hydroarylation of **C** generated the vinylate complex **D**, which on decomposition led to the catalyst and the dihydropyridocoumarin **E**. The latter was oxidized by the air to give the product **22**.

Propargylation of hydroxy pyridocoumarins **18a,b**, **20a,b**, and **22** with propargyl bromide (**6**) (Scheme 5) resulted in propargyloxy derivatives **24a,b**, **25a,b**, and **26**, respectively, in excellent yields (Table 3, entries 6–10). The optimization of the cyclization's conditions was performed for compound **24b**, like in the case of **7b**. The use of Au/TiO$_2$ (4 mol%) in PhCl under microwave irradiation at 180 °C for 2 h gave **27b** in a 99% yield (Table 3, entry 12), while without the catalyst the yield was 95% and no methyl furan derivative was isolated. Propargyloxy derivatives **24a**, **25a,b,** and **26** were also treated with Au/TiO$_2$ (4 mol%) in PhCl to give the pyran derivatives **27a**, **28a,b**, and **29**, respectively, in excellent yields (Table 3, entries 11, 13–15).
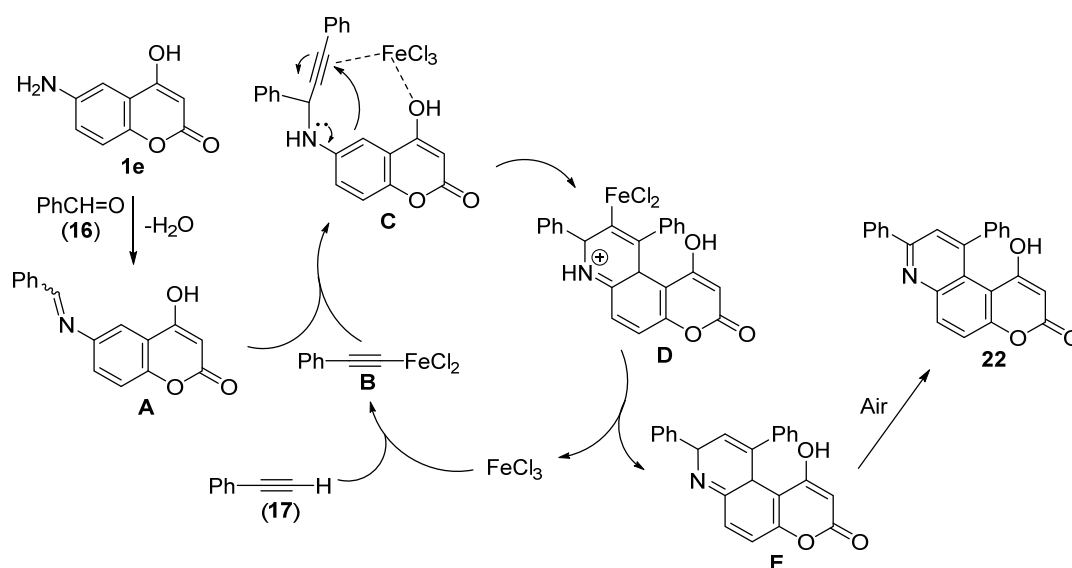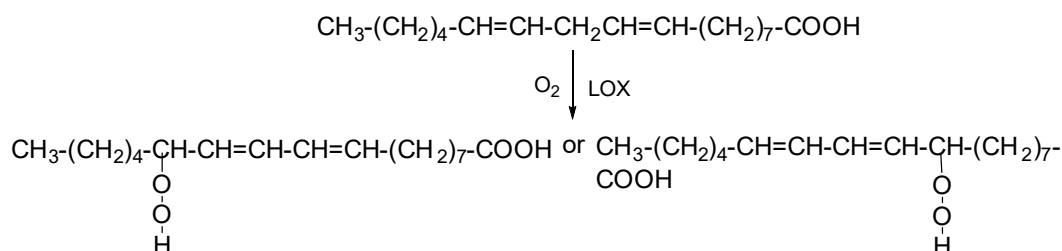
Scheme 6. Possible mechanism for the regioselective synthesis of **22** from **1e**.

2.2. Biology

Preliminary screening biological experiments were performed in vitro. The new fused dipyranoquinolinones **10a,b**, **12a,b**, **14**, **27a,b**, **28a,b**, and **29** were tested as possible inhibitors of EC 1.13.11.12 (linoleate 13S-lipoxygenase) soybean lipoxygenase (LOX) and as antioxidant agents following our previous published assays [39,40,51] (Table 4). Lipoxygenase is a dioxygenase containing non-heme iron. LOX catalyzes the conversion of poly-unsaturated fatty acids with a 1,4-pentadiene system into conjugated hydroperoxy fatty acids (Scheme 7).

Table 4. In vitro antioxidant activity: inhibition of lipid peroxidation (LP). Inhibitory activity of compounds on soybean lipoxygenase (LOX).

Entry	Compound	LOX at 100 μM (%) or IC$_{50}$ (μM)	LP at 100 μM (%)
1	**10a**	no	no
2	**10b**	no	66%
3	**12a**	40%	no
4	**12b**	100 μM	no
5	**14**	100 μM	19%
6	**27a**	82.5 μM	32%
7	**27b**	60 μM	no
8	**28a**	10 μM	41%
9	**28b**	100 μM	70%
10	**29**	85 μM	29%
11	NDGA	0.45 μM	
12	Trolox		91%

$$CH_3\text{-}(CH_2)_4\text{-}CH=CH\text{-}CH_2CH=CH\text{-}(CH_2)_7\text{-}COOH$$

$$O_2 \downarrow LOX$$

$$CH_3\text{-}(CH_2)_4\text{-}\underset{\underset{\underset{H}{O}}{O}}{CH}\text{-}CH=CH\text{-}CH=CH\text{-}(CH_2)_7\text{-}COOH \quad \text{or} \quad CH_3\text{-}(CH_2)_4\text{-}CH=CH\text{-}CH=CH\text{-}\underset{\underset{\underset{H}{O}}{O}}{CH}\text{-}(CH_2)_7\text{-}COOH$$

Scheme 7. The oxygenation of cis-9, cis-12-octadecadienoic acid by lipoxygenase.

Plant lipoxygenases may differ in substrate and product specificities, pH dependence, sensitiveness to inhibitors, stability, amino acid composition, and molecular weight. Compound **28a** presented the most interesting IC_{50} value (10 μM), acting as a lead molecule. The absence of a methyl group leads to a more potent analog compound (**28a**) compared to **28b**. The rest of the molecules are less potent. The anti-lipid peroxidation is medium.

2.3. Docking Studies on Soybean Lipoxygenase

The most active derivative **28a** with IC_{50} = 10 μM was docked to soybean lipoxygenase-1 (3PZW) (Figure 2) selected from the Protein Data Bank (PDB) for being in accordance with the biological protocol. Lipoxygenases catalyze the oxygenation of free and esterified polyunsaturated fatty acids containing a (1-Z, 4-Z)-penta-1,4-diene system to the corresponding hydroperoxy derivatives. They contain a "non-heme" iron per molecule at the substrate-binding site (iron-binding site). Recent research studies have shown that lipoxygenases possess, apart from the substrate-binding site, potential allosteric binding sites [68–70]. Thus, docking studies of compound **28a** to the active site and to the whole protein, so as to encompass all the allosteric sites, were performed. It seems that **28a** interacts with soybean lipoxygenase in an allosteric manner, confirming previous research studies [70,71]. Compound **28a**'s AutoDockVina binding score on SLOX-1 is −11.7 kcal/mol. It develops hydrophobic interactions with Phe143, Val520, Lys526, Pro530, and Trp772 and a π-stacking interaction between the phenyl group and Tyr525. Additionally, two hydrogen bonds are formed between the carbonyl group and Arg182 and the nitrogen of quinolinone and Thr529, and finally a salt bridge with residue His515.
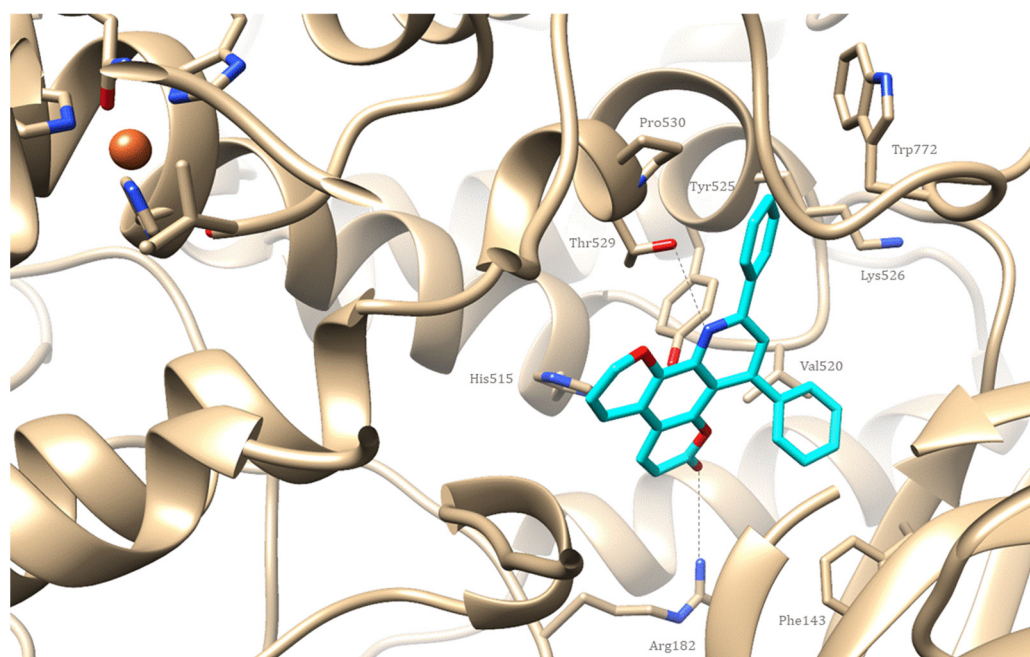

Figure 2. Preferred docking pose of compound **28a** (depicted in cyan) bound on SLOX-1 (3PZW). Blue coloring refers to nitrogen atoms and red to oxygen atoms. Iron appears as an orange sphere.

3. Materials and Methods

3.1. Materials

All the chemicals were purchased from either Sigma-Aldrich Chemie GmbH (Eschenstr. 5, 82024 Taufkirchen, Germany) or Merck KGaA, (Frankfurter Strasse 250, 64293 Darmstadt, Germany). Melting points were determined with a Kofler hotstage apparatus and are uncorrected. IR spectra were obtained with a PerkinElmer Spectrum BX spectrophotometer as KBr pellets. NMR spectra were recorded with an Agilent 500/54 (DD2) (500 MHz and 125 MHz for ^{1}H and ^{13}C, respectively) using TMS as an internal standard. *J* values

are reported in Hz. Mass spectra were determined with an LCMS-2010 EV instrument (Shimadzu, Kyoto, Japan) under electrospray ionization (ESI) conditions. HRMS (ESI-MS) were recorded with a ThermoFisher Scientific (168 Third Avenue, Waltham, MA 02451, USA) model LTQ Orbitrap Discovery MS. Silica gel No. 60 (Merck KGaA, Frankfurter Strasse 250, 64293 Darmstadt, Germany) was used for column chromatography.

3.2. Chemistry

3.2.1. General Procedure for the Synthesis of Methyl-Substituted Pyridine Moiety of Pyranoquinolinones—Synthesis of 6-Hydroxy-8-methyl-3H-pyrano[3,2-f]quinolin-3-one (**3a**)

n-Butyl vinyl ether (**2**) (261.0 μL, 203.5 mg, 2.03 mmol) and iodine (17.2 mg, 0.068 mmol) were added to a solution of 6-amino-7-hydroxycoumarin (**1a**) (0.12 g, 0.68 mmol) in acetonitrile (4 mL). The resulting mixture was refluxed for 1 h. After cooling, the solvent was evaporated and the residue was separated by column chromatography (silica gel No 60, hexane/AcOEt 1:2) to give **3a** (0.145 g, 94% yield).

3a, Yellow Crystals, m.p. 199–200 °C (Ethyl Acetate)

IR (KBr): 3443, 2964, 2927, 1730, 1715, 1552 cm^{-1}. ^{1}H-NMR (500 MHz, CDCl$_3$) δ: 2.75 (s, 3H), 6.37 (d, J = 9.6 Hz, 1H), 7.50 (d, J = 8.6 Hz, 1H), 8.21 (d, J = 9.6 Hz, 1H), 8.36 (d, J = 8.6 Hz, 1H). ^{13}C-NMR (125 MHz, CDCl$_3$) δ: 24.6, 101.1, 106.6, 112.2, 122.3, 124.7, 130.6, 136.5, 138.5, 155.5, 157.1, 161.2. LC–MS (ESI): *m/z* 228 [M + H]$^{+}$, 226 [M − H]$^{-}$. HRMS (ESI): m/z [M + H]$^{+}$ calculated for C$_{13}$H$_{10}$NO$_3$: 228.0660; found: 228.0663.

6-Hydroxy-1,8-dimethyl-3H-pyrano[3,2-f]quinolin-3-one (**3b**)

Mass of 86 mg, 85% yield (from **1b**, 80 mg, 0.42 mmol), yellow crystals, m.p. 153–155 °C (ethyl acetate). IR (KBr): 3350, 2921, 2853, 1715, 1696, 1500 cm^{-1}. ^{1}H-NMR (500 MHz, CDCl$_3$) δ: 2.75 (s, 3H), 2.83 (s, 3H), 6.20 (s, 1H), 7.12 (s, 1H), 7.47 (d, *J* = 8.9 Hz, 1H), 8.80 (d, *J* = 8.9 Hz, 1H). ^{13}C-NMR (125 MHz, CDCl$_3$) δ: 24.3, 25.8, 101.5, 107.0, 113.5, 123.6, 124.1, 133.8, 136.4, 153.6, 155.4, 156.0, 156.2, 160.7.

LC–MS (ESI): *m/z* 273 [M + MeOH]$^{+}$, HRMS (ESI): *m/z* [M + H]$^{+}$ calculated for C$_{14}$H$_{12}$NO$_3$: 242.0817, found: 242.0817.

6-Hydroxy-8-methyl-2H-pyrano[2,3-f]quinolin-2-one (**4a**)

Mass of 73 mg, 98% yield (from **1c**, 60 mg, 0.34 mmol), yellow crystals, m.p. 187–189 °C (ethyl acetate). IR (KBr): 3372, 3059, 2923, 2846, 1729, 1568, 1490 cm^{-1}. ^{1}H-NMR (500 MHz, CDCl$_3$) δ: 2.78 (s, 3H), 6.51 (d, *J* = 9.5 Hz, 1H), 7.07 (s, 1H), 7.48 (d, *J* = 8.5 Hz, 1H), 7.77 (d, *J* = 9.5 Hz, 1H), 8.66 (d, *J* = 8.5 Hz, 1H).

^{13}C-NMR (125 MHz, CDCl$_3$) δ: 25.2, 105.7, 114.8, 116.6, 116.7, 123.7, 131.3, 138.9, 143.9, 144.1, 148.2, 159.9, 160.8. LC–MS (ESI): *m/z* 228 [M + H]$^{+}$, 226 [M − H]$^{-}$. HRMS (ESI): *m/z* [M + H]$^{+}$ calculated for C$_{13}$H$_{10}$NO$_3$: 228.0655, found: 228.0651.

6-Hydroxy-4,8-dimethyl-2H-pyrano[2,3-f]quinolin-2-one (**4b**)

Mass of **80 mg, 85%** yield (from **1d**, 74 mg, 0.39 mmol), yellow crystals, m.p. 180–182 °C (ethyl acetate). IR (KBr): 3383, 3234, 2957, 2923, 2853, 1714, 1640, 1616 cm^{-1}. ^{1}H-NMR (500 MHz, CDCl$_3$) δ: 2.49 (d, *J* = 0.8 Hz, 3H), 2.78 (s, 3H), 6.38 (d, *J* = 0.8 Hz, 1H), 7.22 (s, 1H), 7.48 (d, *J* = 8.6 Hz, 1H), 8.69 (d, *J* = 8.6 Hz, 1H). ^{13}C-NMR (125 MHz, CDCl$_3$) δ: 19.4, 25.1, 102.9, 114.9, 115.8, 116.8, 123.7, 131.7, 138.7, 143.2, 148.1, 153.3, 159.8, 160.9. LC–MS (ESI): *m/z* 242 [M + H]$^{+}$, HRMS (ESI): *m/z* [M + H]$^{+}$ calculated for C$_{14}$H$_{12}$NO$_3$: 242.0812, found: 242.0815.

1-Hydroxy-10-methyl-3H-pyrano[3,2-f]quinolin-3-one (**5**)

Mass of 0.191 g, 99% yield (from **1e**, 0.15 g, 0.85 mmol), yellow crystals, m.p. 177–179 °C (ethyl acetate). IR (KBr): 3357, 2959, 2932, 2873, 1700, 1623, 1569 cm^{-1}. ^{1}H-NMR (500 MHz, CDCl$_3$) δ: 2.76 (s, 3H), 5.58 (s, 1H), 7.41 (d, *J* = 8.9 Hz, 1H), 7.63 (d, *J* = 9.2 Hz, 1H), 8.15 (d, *J* = 9.2 Hz, 1H), 9.38 (d, *J* = 8.9 Hz, 1H). ^{13}C-NMR (125 MHz, CDCl$_3$) δ: 24.7, 100.2, 109.0,

120.6, 123.1, 133.4, 133.5, 134.6, 145.2, 152.2, 157.9, 160.0, 161.8. LC–MS (ESI): m/z 228 [M + H]$^+$. HRMS (ESI): m/z [M + H]+ calculated for $C_{13}H_{10}NO_3$: 228.0655, found: 228.0653.

3.2.2. General Procedure for the Propargylation of Hydroxypyranoquinolinones—Synthesis of 8-Methyl-6-(prop-2-yn-1-yloxy)-3H-pyrano[3,2-f]quinolin-3-one (7a)

Cs_2CO_3 (0.326 g, 1 mmol) and propargyl bromide (**6**) (80% in toluene, (86.3 μL, 0.119 g, 1 mmol)) were added to a solution of 6-hydroxy-8-methyl-3*H*-pyrano[3,2-*f*]quinolin-3-one (**3a**) (0.227 g, 1 mmol) in acetone (4 mL) in a vial for MW oven and the mixture was irradiated at 100 °C for 10 min. The mixture was filtered under reduced pressure and washed with warm acetone (3 × 5 mL). The filtrate was evaporated to give compound **7a** (0.262 g, 99% yield).

7a, Light Yellow Crystals, m.p. 121–123 °C (DCM/Hexane)

IR (KBr): 2927, 2853, 2104, 1712, 1699, 1500 cm^{-1}. ^{1}H-NMR (500 MHz, CDCl$_3$) δ: 2.61 (t, J = 2.4 Hz, 1H), 2.80 (s, 3H), 5.06 (d, J = 2.4 Hz, 2H), 6.45 (d, J = 9.6 Hz, 1H), 7.25 (s, 1H), 7.50 (d, J = 8.6 Hz, 1H), 8.29 (d, J = 9.6 Hz, 1H), 8.38 (d, J = 8.6 Hz, 1H). ^{13}C-NMR (125 MHz, CDCl$_3$) δ: 25.3, 57.2, 77.0, 77.6, 101.4, 107.1, 113.3, 123.2, 124.6, 130.3137.7, 138.7, 154.3, 156.3, 158.5, 161.3. LC–MS (ESI): m/z 266 [M + H]$^+$, 288 [M + Na]$^+$. HRMS (ESI): m/z [M + H]$^+$ calculated for $C_{16}H_{12}NO_3$: 266.0817, found: 266.0819.

1,8-Dimethyl-6-(prop-2-yn-1-yloxy)-3H-pyrano[3,2-f]quinolin-3-one (7b)

Mass of 43 mg, 93% yield (from **3b**, 40 mg, 0.166 mmol), light yellow crystals, m.p. 217–219 °C (DCM/hexane). IR (KBr): 3067, 2971, 2928, 2852, 2117, 1716, 1614, 1580 cm^{-1}. ^{1}H-NMR (500 MHz, CDCl$_3$) δ: 2.60 (t, J = 2.3 Hz, 1H), 2.80 (s, 3H), 2.84 (s, 3H), 5.07 (d, J = 2.3 Hz, 2H), 6.26 (s, 1H), 7.27 (s, 1H), 7.45 (d, J = 8.9 Hz, 1H), 8.80 (d, J = 8.9 Hz, 1H). ^{13}C-NMR (125 MHz, CDCl$_3$) δ: 25.1, 25.9, 57.1, 77.4 102.0, 108.5, 114.5, 123.5, 124.6, 130.0, 133.1, 138.5, 153.4, 154.8, 156.0, 157.2, 160.4. LC–MS (ESI): m/z 302 [M + Na]$^+$. HRMS (ESI): m/z [M + H]$^+$ calculated for $C_{17}H_{14}NO_3$: 280.0973, found: 280.0978.

8-Methyl-6-(prop-2-yn-yloxy)-2H-pyrano[2,3-f]quinolin-2-one (8a)

Mass of 57 mg, 97% yield (from **4a**, 50 mg, 0.22 mmol), light yellow crystals, m.p. 85–87 °C (DCM/hexane). IR (KBr): 2958, 2924, 2853, 2108, 1728, 1615 cm^{-1}. ^{1}H-NMR (500 MHz, CDCl$_3$) δ: 2.57 (t, J = 1.7 Hz, 1H), 2.87 (s, 3H), 5.08 (d, J = 1.7 Hz, 2H), 6.54 (d, J = 9.5 Hz, 1H), 7.22 (s, 1H), 7.51 (d, J = 8.6 Hz, 1H), 7.82 (d, J = 9.5 Hz, 1H), 8.74 (d, J = 8.6 Hz, 1H). ^{13}C-NMR (125 MHz, CDCl$_3$) δ: 25.8, 57.1, 76.7, 78.0, 107.4, 113.8, 116.8, 117.9, 123.8, 131.2, 143.9, 145.6, 149.2, 158.8, 160.5, 161.2.
LC–MS (ESI): m/z 266 [M + H]$^+$. HRMS (ESI): m/z [M + H]$^+$ calculated for $C_{16}H_{12}NO_3$: 266.0812, found: 266.0819.

4,8-Dimethyl-6-(prop-2-yn-1-yloxy)-2H-pyrano[2,3-f]quinolin-2-one (8b)

Mass of 54 mg, 93% yield (from **4b**, 50 mg, 0.207 mmol), light yellow crystals, m.p. 132–134 °C (DCM/hexane). IR (KBr): 3059, 2971, 2928, 2852, 2118, 1715, 1620, 1550 cm^{-1}. ^{1}H-NMR (500 MHz, CDCl$_3$) δ: 2.48 (t, J = 1.75 Hz, 1H), 2.54 (s, 3H), 2.86 (s, 3H), 5.13 (d, J = 1.75 Hz, 2H), 6.39 (s, 1H), 7.13 (s, 1H), 7.49 (d, J = 8.5 Hz, 1H), 8.49 (d, J = 8.5 Hz, 1H). ^{13}C-NMR (125 MHz, CDCl$_3$) δ: 19.9, 25.9, 58.0, 76.2, 82.2, 99.8, 106.5, 114.9, 118.1, 123.6, 131.4, 138.5, 145.4, 148.1, 153.1, 160.7, 161.2. LC–MS (ESI): m/z 280 [M + H]$^+$. HRMS (ESI): m/z [M + Na]$^+$ calculated for $C_{17}H_{13}NaNO_3$: 302.0793, found: 302.0792.

10-Methyl-1-(prop-2-yn-1-yloxy)-3H-pyrano[3,2-f]quinolin-3-one (9)

Mass of 57 mg, 98% yield (from **8**, 50 mg, 0.22 mmol), yellow crystals, m.p. 87–89 °C (ethyl acetate/hexane). IR (KBr): 2927, 2853, 2104, 1710, 1512 cm^{-1}. ^{1}H-NMR (500 MHz, CDCl$_3$) δ: 2.81 (t, J = 2.1 Hz, 1H), 3.2 (s, 3H, CH$_3$), 5.06 (d, J = 2.1 Hz, 2H), 6.1 (s, 1H), 7.77 (d, J = 9.2 Hz, 1H), 7.96 (d, J = 9.3 Hz, 1H), 9.36 (d, J = 9.2 Hz, 1H), 9.89 (d, J = 9.3 Hz, 1H).

^{13}C-NMR (125 MHz, CDCl$_3$) δ: 24.7, 60.1, 77.2, 79.0, 99.9, 109.3, 120.9, 123.1, 133.5, 133.6, 134.8, 145.1, 152.4, 158.0, 161.5, 161.9.

LC–MS (ESI): *m/z* 298 [M + H + MeOH]$^+$. HRMS (ESI): *m/z* [M + H]$^+$ calculated for C$_{16}$H$_{12}$NO$_3$: 266.0817, found: 266.0820.

8,10-Diphenyl-6-(prop-2-yn-1-yloxy)-3H-pyrano[3,2-f]quinolin-3-one (24a)

Mass of 44 mg, 99% yield (from **18a**, 40 mg, 0.11 mmol, 5 min in MW oven), light yellow crystals, m.p. 117–119 °C (DCM/hexane). IR (KBr): 3049, 2958, 2924, 2854, 2116, 1703, 1616, 1546, 1487 cm^{-1}. ^{1}H-NMR (500 MHz, CDCl$_3$) δ: 2.66 (t, *J* = 2.3 Hz, 1H), 5.14 (d, *J* = 2.3 Hz, 2H), 5.91 (d, *J* = 9.6 Hz, 1H), 7.20 (d, *J* = 9.6 Hz, 1H), 7.32 (s, 1H), 7.42–7.46 (m, 2H), 7.47–7.49 (m, 1H), 7.52 (d, *J* = 7.7 Hz, 2H), 7.56–7.58 (m, 3H), 7.88 (s, 1H), 8.21 (d, *J* = 7.2 Hz, 2H). ^{13}C-NMR (125 MHz, CDCl$_3$) δ: 57.4, 77.2, 77.4, 102.5, 107.7, 110.9, 123.1, 123.4, 127.6, 128.5, 128.97, 129.0, 129.5, 129.8, 138.5, 139.7, 141.0, 142.0, 148.2, 155.1, 156.1, 157.0, 160.5. LC–MS (ESI): *m/z* 426 [M + Na]$^+$. HRMS (ESI): *m/z* [M + H]$^+$ calculated for C$_{27}$H$_{18}$NO$_3$: 404.1281, found: 404.1261.

1-Methyl-8,10-diphenyl-6-(prop-2-yn-1-yloxy)-3H-pyrano[3,2-f]quinolin-3-one (24b)

Mass of 40.5 mg, 92% yield (from **18b**, 40 mg, 0.105 mmol, 5 min in MW oven), light yellow crystals, m.p. 123–125 °C (DCM/hexane). IR (KBr): 3054, 2922, 2852, 2124, 1725, 1613, 1537, 1486 cm^{-1}. ^{1}H-NMR (500 MHz, CDCl$_3$) δ: 1.48 (s, 3H), 2.65 (t, *J* = 2.0 Hz, 1H), 5.12 (d, *J* = 2.0 Hz, 2H), 5.88 (s, 1H), 7.25 (s, 1H), 7.43–7.46 (m, 4H), 7.49 (d, *J* = 7.0 Hz, 2H), 7.54 (t, *J* = 7.0 Hz, 2H), 7.94 (s, 1H), 8.24 (d, *J* = 7.5 Hz, 2H). ^{13}C-NMR (125 MHz, CDCl$_3$) δ: 22.6, 57.4, 77.4, 99.4, 101.9, 110.2, 111.7, 121.8, 127.7, 127.9, 128.5, 129.0, 129.1, 129.13, 129.9, 132.2, 138.4, 140.8, 141.8, 148.5, 154.5, 155.2, 156.6, 160.7. LC–MS (ESI): *m/z* 418 [M + H]$^+$. HRMS (ESI): *m/z* [M + H]$^+$ calculated for C$_{28}$H$_{20}$NO$_3$: 418.1438, found: 418.1434.

8,10-Diphenyl-6-(prop-2-yn-1-yloxy)-2H-pyrano[2,3-f]quinolin-2-one (25a)

Mass of 32 mg, 98% yield (from **20a**, 30 mg, 0.082 mmol, 5 min in MW oven), light yellow crystals, m.p. 121–123 °C (DCM/hexane). IR (KBr): 3045, 2958, 2923, 2858, 2116, 1709, 1616, 1546 cm^{-1}. ^{1}H-NMR (500 MHz, CDCl$_3$) δ: 2.59 (t, *J* = 1.9 Hz, 1H), 5.16 (d, *J* = 1.9 Hz, 2H), 6.37 (d, *J* = 9.5 Hz, 1H), 7.44 (d, *J* = 7.8 Hz, 2H), 7.52–7.54 (m, 6H), 7.73 (d, *J* = 9.5 Hz, 1H), 7.90 (s, 1H), 8.25 (d, *J* = 7.8 Hz, 2H). ^{13}C-NMR (125 MHz, CDCl$_3$) δ: 58.1, 76.6, 78.5, 110.0, 114.7, 116.6, 122.7, 127.9, 128.0, 128.1, 128.3, 129.0, 129.2, 130.2, 138.5, 140.7, 143.2, 143.6, 149.2, 150.2, 157.1 (2 x C), 159.2. LC–MS (ESI): *m/z* 404 [M + H]$^+$. HRMS (ESI): *m/z* [M + H]$^+$ calculated for C$_{27}$H$_{18}$NO$_3$: 404.1281, found: 404.1284.

4-Methyl-8,10-diphenyl-6-(prop-2-yn-1-yloxy)-2H-pyrano[2,3-f]quinolin-2-one (25b)

Mass of 42 mg, 95% yield (from **20b**, 40 mg, 0.106 mmol, 5 min in MW oven), light yellow crystals, m.p. 120–122 °C (DCM/hexane). IR (KBr): 3054, 2921, 2853, 2115, 1704, 1614, 1549 cm^{-1}. ^{1}H-NMR (500 MHz, CDCl$_3$) δ: 2.50 (d, 3H), 2.88 (t, *J* = 2.0 Hz, 1H), 5.20 (d, *J* = 2.0 Hz, 2H), 6.25, (s, 1H), 7.41–7.44 (m, 3H), 7.47 (s, 1H), 7.49–7.54 (m, 5H), 7.89 (s, 1H), 8.25 (d, *J* = 7.8 Hz, 2H). ^{13}C-NMR (125 MHz, CDCl$_3$) δ: 19.52, 58.5, 76.6, 78.6, 107.9, 115.1, 115.7, 116.9, 122.7, 127.8, 128.02, 128.04, 128.2, 129.0, 130.1, 138.5, 141.0, 146.2, 149.5, 150.0, 152.1, 153.4, 157.1, 159.2. LC–MS (ESI): *m/z* 440 [M + Na]$^+$. HRMS (ESI): *m/z* [M + H]$^+$ calculated for C$_{28}$H$_{20}$NO$_3$: 418.1438, found: 418.1440.

8,10-Diphenyl-1-(prop-2-yn-1-yloxy)-3H-pyrano[3,2-f]quinolin-3-one (26)

Mass of 47 mg, 98% yield (from **22**, 45 mg, 0.123 mmol, 5 min in MW oven), light yellow crystals, m.p. 129–131 °C (DCM/hexane). IR (KBr): 3050, 2921, 2853, 2113, 1715, 1621, 1545 cm^{-1}. ^{1}H-NMR (500 MHz, CDCl$_3$) δ: 2.58 (t, *J* = 2.2 Hz, 1H), 4.68 (d, *J* = 2.2 Hz, 2H), 5.75 (s, 1H), 7.20–7.24 (m, 3H), 7.29 (t, *J* = 8.0 Hz, 4H), 7.42 (d, *J* = 8.0 Hz, 2H), 7.47–7.50 (m, 3H), 7.83 (d, *J* = 9.2 Hz, 1H). ^{13}C-NMR (125 MHz, CDCl$_3$) δ: 51.7 74.7, 77.8, 109.6, 112.7, 117.1, 120.8, 124.3, 126.8, 128.1, 128.29, 128.32, 128.7, 129.7, 129.8, 130.5, 137.1, 152.4, 153.1,

156.9, 157.6, 162.9, 172.9. LC–MS (ESI): *m/z* 404 [M + H]⁺. HRMS (ESI): *m/z* [M + H]⁺ calculated for $C_{27}H_{18}NO_3$: 404.1281, found: 404.1286.

3.2.3. General Procedure for the Synthesis of Diphenyl-Substituted Pyridine Moiety of Pyranoquinolinones—Synthesis of 6-Hydroxy-8,10-diphenyl-3H-pyrano[3,2-f]quinolin-3-one (**18a**) and 2-Phenyl-6H-chromeno[6,7-d]oxazol-6-one (**19a**)

Benzaldehyde (**16**) (48 mg, 0.452 mmol) was added to a solution of **1a** (80 mg, 0.452 mmol) in toluene (5 mL) followed by the addition of phenylacetylene (**17**) (54.6 μL, 52.7 mg, 0.452 mmol) and FeCl₃·6H₂O (7.3 mg, 0.045 mmol). The resulting mixture was refluxed for 24 h. After cooling, the solvent was evaporated and the residue was separated by column chromatography (silica gel No 60, hexane/AcOEt 2:1) to give **18a** (0.109 g, 66% yield) followed by **19a** (38 mg, 32% yield).

18a, Yellow Crystals, m.p. 150–152 °C (Ethyl Acetate/Hexane)

IR (KBr): 3442, 2926, 2853, 1712, 1699, 1500 cm⁻¹. ¹H-NMR (500 MHz, CDCl₃) δ: 5.88 (d, *J* = 10.0 Hz, 1H), 7.18 (d, *J* = 10.0 Hz, 1H), 7.20 (s, 1H), 7.43–7.45 (m, 2H), 7.52–7.53 (m, 1H), 7.55 (d, *J* = 7.5 Hz, 2H), 7.56–7.60 (m, 3H), 7.90 (s, 1H), 8.15 (d, *J* = 7.5 Hz, 2H). ¹³C-NMR (125 MHz, CDCl₃) δ: 101.9, 106.4, 110.4, 112.3, 124.0, 127.3, 128.4, 129.1, 129.2, 129.5, 130.2, 137.2, 137.3, 140.4, 141.7, 149.2, 153.8, 156.0, 157.4, 160.6. LC–MS (ESI): *m/z* 366 [M + H]⁺, 364 [M − H]⁻. HRMS (ESI): *m/z* [M + Na]⁺ calculated for $C_{24}H_{15}NaNO_3$: 388.0950, found: 388.0950.

19a, Yellow Crystals, m.p. 210–211 °C (MeOH) (Lit. [66], m.p. 207–209 °C)
6-Hydroxy-1-methyl-8,10-diphenyl-3H-pyrano[3,2-f]quinolin-3-one (**18b**)

Mass of 0.159 g, 62% yield (from **1b**, 0.13 g, 0.68 mmol), yellow crystals, m.p. 177–179 °C (ethyl acetate/hexane). IR (KBr): 3297, 3058, 2980, 2919, 2857, 1721, 1629, 1529, 1483 cm⁻¹. ¹H-NMR (500 MHz, CDCl₃) δ: 1.45 (s, 3H), 5.86 (s, 1H), 7.13 (s, 1H), 7.46–7.54 (m, 5H), 7.53 (t, *J* = 7.3 Hz, 1H), 7.57 (t, *J* = 7.3 Hz, 2H), 7.99 (s, 1H), 8.19 (d, *J* = 7.3 Hz, 2H). ¹³C-NMR (125 MHz, CDCl₃) δ: 22.7, 101.4, 108.8, 111.2, 122.6, 122.7, 127.3, 128.4, 129.1, 129.2, 129.5, 130.2, 137.3, 138.8, 141.6, 149.5, 154.31, 154.32, 155.6, 156.7, 160.7. LC–MS (ESI): *m/z* 418 [M + K]⁺. HRMS (ESI): *m/z* [M + H]⁺ calculated for $C_{25}H_{18}NO_3$: 380.1286, found: 380.1285.

8-Methyl-2-phenyl-6H-chromeno[6,7-d]oxazol-6-one (**19b**)

Mass of 66 mg, 35% yield (from **1b**, 0.13 g, 0.68 mmol), light yellow crystals, m.p. 231–232 °C (MeOH) (lit. [66], m.p. 232–233 °C).

6-Hydroxy-8,10-diphenyl-2H-pyrano[2,3-f]quinolin-2-one (**20a**)

Mass of 40 mg, 65% yield (from **1c**, 30 mg, 0.17 mmol), yellow crystals, m.p. 207–209 °C (ethyl acetate/hexane). IR (KBr): 3460, 2958, 2922, 2853, 1726, 1635, 1616 cm⁻¹. ¹H-NMR (500 MHz, CDCl₃) δ: 6.38 (d, *J* = 9.5 Hz, 1H), 7.18 (s, 1H), 7.47 (d, *J* = 7.5 Hz, 2H), 7.55 (t, *J* = 7.5 Hz, 6H), 7.71 (d, 1H, *J* = 9.5 Hz), 7.92 (s, 1H), 8.21 (d, 2H, *J* = 7.5 Hz). ¹³C-NMR (125 MHz, CDCl₃) δ: 106.6, 116.0, 116.9, 123.1, 127.7, 127.8, 128.1, 128.2, 128.5, 129.0, 129.1, 130.5, 137.6, 140.1, 140.3, 143.6, 148.9, 150.0, 156.0, 159.4. LC–MS (ESI): *m/z* 388 [M + Na]⁺, 364 [M − H]⁻. HRMS (ESI): *m/z* [M + H]⁺ calculated for $C_{24}H_{15}NO_3$: 366.1125, found: 366.1129.

2-Phenyl-6H-chromeno[7,6-d]oxazol-6-one (**21a**)

Mass of 13 mg, 29% yield (from **1c**, 30 mg, 0.17 mmol), light yellow crystals, m.p. 207–209 °C (ethyl acetate/hexane). IR (KBr): 3076, 2922, 2847, 1725 cm⁻¹. ¹H-NMR (500 MHz, CDCl₃) δ: 6.47 (d, *J* = 9.6 Hz, 1H), 7.56 (t, *J* = 7.7 Hz, 2H), 7.59–7.61 (m, 1H), 7.66 (s, 1H), 7.72 (s, 1H), 7.81 (d, *J* = 9.6 Hz, 1H), 8.29 (d, *J* = 7.7 Hz, 2H). ¹³C-NMR (125 MHz, CDCl₃) δ: 107.7, 108.2, 116.1, 116.5, 126.3, 128.2, 129.2, 132.6, 143.5, 145.3, 147.5, 151.8, 160.7, 166.4. LC–MS (ESI): *m/z* 264 [M + H]⁺. HRMS (ESI): *m/z* [M + H]⁺ calculated for $C_{16}H_{10}NO_3$: 264.0655, found: 264.0657.

6-Hydroxy-4-methyl-8,10-diphenyl-2H-pyrano[2,3-f]quinolin-2-one (**20b**)

Mass of 93 mg, 63% yield (from **1d**, 74 mg, 0.39 mmol), light yellow crystals, m.p. 185–187 °C (ethyl acetate/hexane). IR (KBr): 3371, 3059, 2958, 2923, 2857, 1725, 1548 cm^{-1}. ^{1}H-NMR (500 MHz, CDCl$_3$) δ: 2.47 (s, 3H), 6.26 (s, 1H), 7.38 (s, 1H), 7.45 (d, *J* = 7.1 Hz, 2H), 7.55 (m, 6H), 7.91 (s, 1H), 8.20 (d, *J* = 7.1 Hz, 2H), 8.78 (br.s, 1H, OH). ^{13}C-NMR (125 MHz, CDCl$_3$) δ: 19.7, 104.3, 115.4, 115.9, 117.1, 123.2, 127.8, 128.1, 128.2, 128.5, 129.1, 130.7, 137.1, 139.6, 140.2, 143.9, 148.4, 150.7, 152.4, 155.8, 159.3. LC–MS (ESI): *m/z* 380 [M + H]$^+$, 378 [M − H]$^-$. HRMS (ESI): *m/z* [M + H]$^+$ calculated for C$_{25}$H$_{18}$NO$_3$: 380.1281, found: 380.1271.

8-Methyl-2-phenyl-6H-chromeno[7,6-d]oxazol-6-one (**21b**)

Mass of 36 mg, 33% yield (from **1d**, 74 mg, 0.39 mmol), light yellow crystals, m.p. 160–162 °C (ethyl acetate/hexane). IR (KBr): 3064, 2920, 2852, 1722, 1704, 1619, 1604 cm^{-1}. ^{1}H NMR (500 MHz, CDCl$_3$) δ: 2.51 (s, 3H, CH$_3$), 6.33 (s, 1H), 7.54–7.57 (m, 2H), 7.59 (m, 1H), 7.69 (s, 1H), 7.76 (s, 1H), 8.26 (d, *J* = 7.0 Hz, 2H). ^{13}C-NMR (125 MHz, CDCl$_3$) δ: 19.2, 105.2, 107.6, 114.7, 117.8, 126.3, 128.1, 129.1, 132.5, 145.0, 147.5, 151.2, 152.0, 160.7, 166.3. LC–MS (ESI): *m/z* 332 [M + Na + MeOH]$^+$. HRMS (ESI): *m/z* [M + H]$^+$ calculated for C$_{17}$H$_{12}$NO$_3$: 278.0812, found: 278,0820.

1-Hydroxy-8,10-diphenyl-3H-pyrano[3,2-f]quinolin-3-one (**22**)

Mass of 0.253 g, 82% yield (from **1e**, 0.15 g, 0.845 mmol), yellow crystals, m.p. 203–205 °C (ethyl acetate/hexane). IR (KBr): 3445, 2952, 2928, 2857, 1715, 1459 cm^{-1}. ^{1}H-NMR (500 MHz, CDCl$_3$) δ: 5.79 (s, 1H), 7.28–7.32 (m, 3H), 7.35–7.39 (m, 4H), 7.46–7.56 (m, 3H), 7.62 (d, *J* = 7.7 Hz, 2H), 8.12 (d, *J* = 9.2 Hz, 1H). ^{13}C-NMR (125 MHz, CDCl$_3$) δ: 86.5, 104.9, 115.8, 116.3, 121.5, 123.2, 123.9, 127.0, 127.4, 128.2, 128.3, 128.7, 128.9, 131.6, 132.2, 138.4, 152.5, 161.0, 162.5, 178.2. LC–MS (ESI): *m/z* 388 [M + Na]$^+$. HRMS (ESI): *m/z* [M + H]$^+$ calculated for C$_{24}$H$_{16}$NO$_3$: 366.1125, found: 366.1128.

2,4,10,12-Tetraphenyl-4H,5H-pyrano[2′,3′:4,5]pyrano[3,2-f]quinolin-5-one (**23**)

Mass of 47 mg, 10% yield (eluted before **22**; from **1e**, 0.15 g, 0.845 mmol), yellow oil. IR (KBr): 3955, 2923, 2854, 1721 cm^{-1}. ^{1}H-NMR (500 MHz, CDCl$_3$) δ: 4.72 (d, *J* = 4.9 Hz, 1H), 5.85 (d, *J* = 4.9 Hz, 1H), 7.23 (t, *J* = 7.3 Hz, 2H), 7.31 (d, *J* = 7.9 Hz, 2H), 7.34 (d, *J* = 7.9 Hz, 2H), 7.36–7.40 (m, 2H), 7.41–7.47 (m, 6H), 7.57 (t, *J* = 7.3 Hz, 2H), 7.74 (d, *J* = 7.3 Hz, 2H), 8.03 (d, *J* = 7.9 Hz, 1H). ^{13}C-NMR (125 MHz, CDCl$_3$) δ: 36.7, 103.7, 103.8, 114.6, 116.9, 122.7, 124.2, 124.7, 127.3, 128.5, 128.67, 128.71, 129.3, 132.0, 132.7, 141.1, 143.6, 146.3, 146.9, 152.78, 152.80, 155.8, 156.0, 161.5, 163.1. LC–MS (ESI): *m/z* 578 [M + Na]$^+$.

3.2.4. General Procedure for the Preparation of Pyran Derivatives via the 6-Endo-Dig Cyclization of Propargyloxy Derivatives—Synthesis of 11-Methyl-2H,6H-dipyrano[3,2-f:3′,2′-h] quinolin-6-one (**10a**)

A mixture of **7a** (45 mg, 0.17 mmol) and Au/TiO$_2$ (0.134 g of 1%, 1.34 mg Au, 0.00679 mmol, 4 mol%) in chlorobenzene (4 mL) was irradiated under MW irradiation at 180 °C for 2 h. After the filtration of the catalyst through a silica gel layer, the solvent was evaporated and the residue was separated by column chromatography (silica gel No 60, hexane/AcOEt (2:1→1:1)) to give compound **10a** (43 mg, 96% yield).

10a, Light Yellow Crystals, m.p. 101–103 °C (DCM/Hexane)

IR (KBr): 3029, 2925, 2858, 1719, 1542 cm^{-1}. ^{1}H-NMR (500 MHz, CDCl$_3$) δ: 2.85 (s, 3H), 5.26 (d, *J* = 3.5 Hz, 2H), 5.99 (dt, *J$_1$* = 3.5 Hz, *J$_2$* = 10.1 Hz, 1H), 6.53 (d, *J* = 9.8 Hz, 1H), 7.53 (d, *J* = 8.6 Hz, 1H), 8.27 (d, *J* = 9.8 Hz, 1H), 8.35 (d, *J* = 8.6 Hz, 1H). ^{13}C-NMR (125 MHz, CDCl$_3$) δ: 25.1, 67.9, 108.7, 111.2, 114.4, 118.3, 122.1, 123.4, 124.3, 133.0, 137.5, 143.5, 150.3, 150.4, 157.5, 160.9. LC–MS (ESI): *m/z* 288 [M + Na]$^+$. HRMS (ESI): *m/z* [M + H]$^+$ calculated for C$_{16}$H$_{12}$NO$_3$: 266.0812, found: 266.0815.

8,11-Dimethyl-2H,6H-dipyrano[3,2-f:3′,2′-h]quinolin-6-one (10b)

Mass of 42 mg, 93% yield (from **7b**, 45 mg, 0.161 g), yellow crystals, m.p. 96–98 °C (DCM/hexane). IR (KBr): 3024, 2925, 2853, 1721, 1546 cm^{-1}. ^{1}H-NMR (500 MHz, CDCl$_3$) δ: 2.79 (s, 3H), 2.83 (s, 3H), 5.24 (dd, J_1 = 2.0 Hz, J_2 = 3.5 Hz, 2H), 5.98 (dt, J_1 = 3.5 Hz, J_2 = 10.1 Hz, 1H), 6.25 (s, 1H), 7.12 (d, J = 10.1 Hz, 1H), 7.38 (d, J = 9.0 Hz, 1H), 8.74 (d, J = 9.0 Hz, 1H). ^{13}C-NMR (125 MHz, CDCl$_3$) δ: 25.1, 26.1, 67.1, 108.0, 111.0, 114.2, 118.3, 122.0, 123.2, 124.2, 133.2, 137.2, 150.3, 150.4, 153.7, 157.5, 160.2. LC–MS (ESI): *m/z* 312 [M + H +MeOH]$^+$. HRMS (ESI): *m/z* [M + Na]$^+$ calculated for C$_{17}$H$_{13}$NaNO$_3$: 302.0788, found: 302.0787.

2-Methyldipyrano[2,3-f:3′,2′-h]quinolin-6(11H)-one (12a)

Mass of 48 mg, 96% yield (from **8a**, 50 mg, 0.189 mmol), light yellow crystals, m.p. 95–97 °C (DCM/hexane). IR (KBr): 3060, 2928, 2852, 1718, 1570 cm^{-1}. ^{1}H-NMR (500 MHz, CDCl$_3$) δ: 2.87 (s, 3H), 5.12 (d, J = 2.1 Hz, 2H), 6.12 (dt, J_1 = 3.5 Hz, J_2 = 9.9 Hz), 6.57 (d, J = 9.7 Hz, 1H), 6.86 (d, J = 9.9 Hz, 1H), 7.44 (d, J = 8.6 Hz, 1H), 8.01 (d, J = 9.7 Hz, 1H), 8.71 (d, J = 8.6 Hz, 1H). ^{13}C-NMR (125 MHz, CDCl$_3$) δ: 24.9, 68.1, 108.0, 111.2, 114.7, 118.1, 122.6, 123.5, 124.2, 133.4, 137.4, 143.7, 150.3, 150.5, 157.8, 161.2. LC–MS (ESI): *m/z* 266 [M + H]$^+$. HRMS (ESI): *m/z* [M + Na]$^+$ calculated for C$_{16}$H$_{11}$NaNO$_3$: 288.0637, found: 288.0640.

2,8-Dimethyldipyrano[2,3-f:3′,2′-h]quinolin-6(11H)-one (12b)

Mass of 41 mg, 91% yield (from 8b, 45 mg, 0.161 mmol), yellow crystals, m.p. 89–91 °C (DCM/hexane). IR (KBr): 3029, 2924, 2853, 1718, 1547 cm^{-1}. ^{1}H-NMR (500 MHz, CDCl$_3$) δ: 2.75 (s, 3H), 2.80 (s, 3H), 5.29 (dd, J_1 = 2.1 Hz, J_2 = 3.4 Hz, 2H), 6.00 (dt, J_1 = 3.4 Hz, J_2 = 10.0 Hz, 1H), 6.27 (s, 1H), 7.15 (d, J = 10.0 Hz, 1H), 7.40 (d, J = 9.3 Hz, 1H), 8.75 (d, J = 9.3 Hz, 1H). ^{13}C-NMR (125 MHz, CDCl$_3$) δ: 25.0, 26.4, 67.9, 108.5, 110.8, 113.8, 118.1, 121.8, 123.2, 124.1, 133.3, 137.0, 150.3, 150.4, 153.9, 157.1, 161.2. LC–MS (ESI): *m/z* 280 [M + H]$^+$. HRMS (ESI): *m/z* [M + Na]$^+$ calculated for C$_{17}$H$_{13}$NaNO$_3$: 302.0788, found: 302.0790.

12-Methyl-4H,5H-pyrano[2′,3′:4,5]pyrano[3,2-f]quinolin-5-one (14)

Mass of 47 mg, 94% yield (from **9**, 50 mg, 0.189 mmol), light yellow crystals, m.p. 111–113 °C (DCM/hexane). IR (KBr): 3025, 2929, 2854, 1718, 1545 cm^{-1}. ^{1}H-NMR (500 MHz, CDCl$_3$) δ: 2.69 (s, 3H), 4.69 (d, J = 3.7 Hz, 2H), 5.99 (dt, J_1 = 3.7 Hz, J_2 = 9.9 Hz, 1H), 6.55 (d, J = 9.9 Hz, 1H), 7.75 (d, J = 9.2 Hz, 1H), 8.01 (d, J = 9.3 Hz, 1H), 9.30 (d, J = 9.2 Hz, 1H), 9.85 (d, J = 9.3 Hz, 1H). ^{13}C-NMR (125 MHz, CDCl$_3$) δ: 24.7, 73.4, 109.3, 111.1, 118.3, 120.9, 123.1, 133.5, 133.6, 134.8, 145.1, 145.2, 151.4, 152.5, 161.5, 161.9. LC–MS (ESI): *m/z* 288 [M + Na]$^+$. HRMS (ESI): *m/z* [M + H]$^+$ calculated for C$_{16}$H$_{12}$NO$_3$: 266.0812, found: 266.0815.

9,11-Diphenyl-2H,6H-dipyrano[3,2-f:3′,2′-h]quinolin-6-one (27a)

Mass of 34 mg, 97% yield (from **24a**, 35 mg, 0.087 mmol), light yellow crystals, m.p. 165–167 °C (DCM/hexane). IR (KBr): 2927, 2854, 1705, 1682, 1619 cm^{-1}. ^{1}H-NMR (500 MHz, CDCl$_3$) δ: 5.25 (d, J = 3.6 Hz, 2H), 5.97 (d, J = 9.9 Hz, 1H), 6.03 (dt, J_1 = 3.6 Hz, J_2 = 10.1 Hz, 1H), 7.11 (d, J = 10.1 Hz, 1H), 7.20 (d, J = 9.9 Hz, 1H), 7.42–7.45 (m, 2H), 7.48 (d, J = 7.7 Hz, 2H), 7.52 (t, J = 7.7 Hz, 2H), 7.56–7.58 (m, 2H), 7.90 (s, 1H), 8.20 (d, J = 7.7 Hz, 2H). ^{13}C-NMR (125 MHz, CDCl$_3$) δ: 69.2, 109.6, 111.0, 111.5, 118.7, 121.5, 121.7, 123.0, 127.7, 128.9, 129.0, 129.6, 138.4, 140.0, 140.8, 141.6, 143.2, 148.4, 151.1, 152.9, 155.1, 155.9, 160.9. LC–MS (ESI):*m/z* 404 [M + H]$^+$. HRMS (ESI): *m/z* [M + H]$^+$ calculated for C$_{27}$H$_{18}$NO$_3$: 404.1281, found: 404.1283.

8-Methyl-9,11-diphenyl-2H,6H-dipyrano[3,2-f:3′,2′-h]quinolin-6-one (27b)

Mass of 25 mg, 99% yield (from **24b**, 25 mg, 0.06 mmol), light yellow crystals, m.p. 170–172 °C (DCM/hexane). IR (KBr): 2933, 2854, 1699, 1682, 1621 cm^{-1}. ^{1}H-NMR (500 MHz, CDCl$_3$) δ: 1.49 (s, 3H), 5.28 (d, J = 3.6 Hz, 2H), 5.87 (s, 1H), 6.00 (dt, J_1 = 3.6 Hz, J_2 = 10.0 Hz, 1H), 7.12 (d, J = 10.0 Hz, 1H), 7.43–7.47 (m, 3H), 7.48 (d, J = 7.5 Hz, 2H), 7.54 (t,

J = 7.5 Hz, 3H), 7.87 (s, 1H), 8.21 (d, *J* = 7.5 Hz, 2H). ^{13}C-NMR (125 MHz, CDCl$_3$) δ: 29.7, 67.0, 109.8, 110.9, 111.2, 118.4, 121.6, 121.7, 122.9, 127.6, 128.9, 129.0, 129.7, 138.6, 139.9, 140.6, 141.9, 148.2, 151.1, 153.19, 153.20, 154.8, 155.9, 160.5. LC–MS (ESI): *m/z* 440 [M + Na]$^+$. HRMS (ESI): *m/z* [M + H]$^+$ calculated for C$_{28}$H$_{20}$NO$_3$: 418.1428, found: 418.1434.

2,4-Diphenyldipyrano[2,3-f:3′,2′-h]quinolin-6(11H)-one (**28a**)

Mass of 38 mg, 96% yield (from **25a**, 40 mg, 0.099 mmol), light yellow crystals, m.p. 93–95 °C (DCM/hexane). IR (KBr): 2930, 2852, 1716, 1682, 1623 cm^{-1}. ^{1}H-NMR (500 MHz, CDCl$_3$) δ: 5.23 (d, *J* = 3.4 Hz, 2H), 6.03 (dt, *J$_1$* = 3.4 Hz, *J$_2$* = 10.0 Hz, 1H), 6.39 (d, *J* = 9.5 Hz, 1H), 6.81 (d, *J* = 10.0 Hz, 1H), 7.47 (d, *J* = 7.9 Hz, 2H), 7.52–7.55 (m, 6H), 7.71 (d, *J* = 9.5 Hz, 1H), 7.91 (s, 1H), 8.28 (d, *J* = 7.9 Hz, 2H). ^{13}C-NMR (125 MHz, CDCl$_3$) δ: 71.0, 110.6, 111.1, 111.8, 119.2, 121.5, 121.7, 123.4, 127.9, 128.9, 129.0, 129.5, 138.6, 139.9, 140.7, 141.1, 143.2, 148.6, 151.2, 153.0, 155.1, 156.4, 161.4. LC–MS (ESI): *m/z* 404 [M + H]$^+$. HRMS (ESI): *m/z* [M + H]$^+$ calculated for C$_{27}$H$_{18}$NO$_3$: 404.1281, found: 404.1285.

8-Methyl-2,4-diphenyldipyrano[2,3-f:3′,2′-h]quinolin-6(11H)-one (**28b**)

Mass of 37 mg, 93% yield (from **25b**, 40 mg, 0.096 mmol), light yellow crystals, m.p. 175–177 °C (DCM/hexane). IR (KBr): 3062, 2918, 2853, 1732, 1583 cm^{-1}. ^{1}H-NMR (500 MHz, CDCl$_3$) δ: 2.60 (s, 3H), 4.98 (d, *J* = 4.4 Hz, 2H), 6.01–6.06 (m, 1H), 6.21 (s, 1H), 7.02 (d, *J* = 9.6 Hz, 2H), 7.41 (d, *J* = 7.2 Hz, 2H), 7.49–7.53 (m, 5H), 7.83 (s, 1H), 8.22 (d, *J* = 7.2 Hz, 2H). ^{13}C-NMR (125 MHz, CDCl$_3$) δ: 29.5, 72.0, 110.1, 110.9, 111.4, 118.8, 121.5, 121.8, 123.0, 127.7, 128.7, 129.0, 129.5, 138.5, 140.0, 140.9, 141.5, 148.4, 151.5, 153.18, 153.2, 155.0, 155.8, 160.9. LC–MS (ESI): *m/z* 440 [M + Na]$^+$. HRMS (ESI): *m/z* [M + H]$^+$ calculated for C$_{28}$H$_{20}$NO$_3$: 418.1428, found: 418.1431.

10,12-Diphenyl-2H,5H-pyrano[2′,3′:4,5]pyrano[3,2-f]quinolin-5-one (**29**)

Mass of 46 mg, 92% yield (from **26**, 50 mg, 0.124 mmol), light yellow crystals, m.p. 152–154 °C (DCM/hexane). IR (KBr): 2929, 2854, 1705, 1684, 1618 cm^{-1}. ^{1}H-NMR (500 MHz, CDCl$_3$) δ: 4.68 (d, *J* = 3.1 Hz, 2H), 6.01 (dt, *J$_1$* = 3.1, *J$_2$* = 9.9 Hz, 1H), 6.57 (d, *J* = 9.9 Hz, 1H), 7.22–7.24 (m, 3H), 7.31 (t, *J* = 8.0 Hz, 4H), 7.45 (d, *J* = 8.0 Hz, 2H), 7.47–7.50 (m, 3H), 7.82 (d, *J* = 7.8 Hz, 1H). ^{13}C-NMR (125 MHz, CDCl$_3$) δ: 72.1, 109.6, 112.7, 117.1, 118.7, 120.7, 124.0, 126.9, 128.2, 128.29, 128.32, 128.8, 129.7, 129.8, 130.6, 137.2, 140.2, 144.9, 153.1, 156.9, 157.6, 162.9, 172.9. LC–MS (ESI): *m/z* 404 [M + H]$^+$. HRMS (ESI): *m/z* [M + Na]$^+$ calculated for C$_{27}$H$_{17}$NaNO$_3$: 426.1101, found: 426.1104.

3.2.5. General Procedure for the Preparation of Furan Derivatives via the 5-Exo-Dig Cyclization of Propargyloxy Derivatives—Synthesis of 2,10-Dimethyl-5H-furo[3,2-h] pyrano[3,2-f]quinolin-5-one (**11a**)

A solution of **7a** (65 mg, 0.245 mmol) in PhCl (4 mL) was irradiated under MW irradiation at 180 °C for 2.5 h. After cooling the residue was purified by column chromatography (silica gel No 60, hexane/AcOEt (2:1)) to give compound **11a** (59 mg, 90% yield).

11a, Light Yellow Crystals, m.p. 97–99 °C (DCM/Hexane)

IR (KBr): 3056, 2923, 2852, 1721, 1576 cm^{-1}. ^{1}H-NMR (500 MHz, CDCl$_3$) δ: 2.66 (s, 3H), 2.85 (s, 3H), 6.53 (d, *J* = 9.8 Hz, 1H), 6.88 (s, 1H), 7.45 (d, *J* = 8.6 Hz, 1H), 8.39 (d, *J* = 9.8 Hz, 1H), 8.44 (d, *J* = 8.6 Hz, 1H). ^{13}C-NMR (125 MHz, CDCl$_3$) δ: 14.5, 25.2, 101.4, 108.4, 113.8, 119.71, 119.74, 122.3, 130.6, 134.3, 139.4, 148.3, 157.1, 158.0, 158.9, 160.7. LC–MS (ESI): *m/z* 266 [M + H]$^+$. HRMS (ESI): *m/z* [M + H]$^+$ calculated for C$_{16}$H$_{12}$NO$_3$: 266.0812, found: 266.0817.

2,7,10-Trimethyl-5H-furo[3,2-h]pyrano[3,2-f]quinolin-5-one (**11b**)

Mass of 44 mg, 98% yield (from **7b**, 45 mg, 0.161 mmol), yellow crystals, m.p. 96–98 °C (DCM/hexane). IR (KBr): 3053, 2925, 2850, 1718, 1573 cm^{-1}. ^{1}H-NMR (500 MHz, CDCl$_3$) δ: 2.66 (s, 3H), 2.84 (s, 3H), 2.91 (s, 3H), 6.35 (s, 1H), 6.90 (s, 1H), 7.39 (d, *J* = 9.0 Hz, 1H), 8.87 (d, *J* = 9.0 Hz, 1H). ^{13}C-NMR (125 MHz, CDCl$_3$) δ: 13.9, 22.1, 25.6, 101.5, 108.7, 114.0,

119.7, 119.8, 122.4, 131.1, 134.2, 139.5, 148.3, 157.2, 158.0, 158.8, 161.2. LC–MS (ESI): m/z 280 [M + H]$^+$. HRMS (ESI): m/z [M + H]$^+$ calculated for $C_{17}H_{14}NO_3$: 280.0974, found: 280.0978.

2,10-Dimethyl-6H-furo[3,2-h]pyrano[2,3-f]quinolin-6-one (**13a**)

Mass of 38 mg, 95% yield (from **8a**, 40 mg, 0.151 mmol), light yellow crystals, m.p. 100–102 °C (DCM/hexane). IR (KBr): 3055, 2926, 2852, 1715, 1573 cm^{-1}. ^{1}H-NMR (500 MHz, CDCl$_3$) δ: 2.64 (s, 3H), 2.85 (s, 3H), 6.52 (d, J = 9.9 Hz, 1H), 6.89 (s, 1H), 7.48 (d, J = 8.6 Hz, 1H), 8.35 (d, J = 9.9 Hz, 1H), 8.46 (d, J = 8.6 Hz, 1H). ^{13}C-NMR (125 MHz, CDCl$_3$) δ: 14.3, 25.0, 101.7, 108.3, 113.7, 119.72, 119.74, 122.5, 130.8, 134.0, 139.5, 148.4, 157.0, 158.1, 159.0, 161.3. LC–MS (ESI): m/z 266 [M + H]$^+$. HRMS (ESI): m/z [M + H]+ calculated for $C_{16}H_{12}NO_3$: 266.0812, found: 266.0813.

2,8,10-Trimethyl-6H-furo[3,2-h]pyrano[2,3-f]quinolin-6-one (**13b**)

Mass of 39 mg, 93% yield (from **8b**, 42 mg, 0.15 mmol), yellow crystals, m.p. 97–99 °C (DCM/hexane). IR (KBr): 3058, 2923, 2857, 1719, 1546 cm^{-1}. ^{1}H-NMR (500 MHz, CDCl$_3$) δ: 2.67 (s, 3H), 2.79 (s, 3H), 2.91 (s, 3H), 6.33 (s, 1H), 6.93 (s, 1H), 7.41 (d, J = 9.0 Hz, 1H), 8.85 (d, J = 9.0 Hz, 1H). ^{13}C-NMR (125 MHz, CDCl$_3$) δ: 13.7, 21.8, 25.4, 101.3, 108.9, 114.2, 119.7, 119.8, 121.9, 131.4, 134.1, 139.8, 148.4, 157.0, 158.2, 158.6, 161.1. LC–MS (ESI): m/z 280 [M + H]$^+$. HRMS (ESI): m/z [M + Na]$^+$ calculated for $C_{17}H_{13}NaNO_3$: 302.0788, found: 302.0791.

2,11-Dimethyl-4H-furo[2′,3′:4,5]pyrano[3,2-f]quinolin-4-one (**15**)

Mass of 37 mg, 93% yield (from **9**, 50 mg, 0.151 mmol), light yellow crystals, m.p. 112–114 °C (DCM/hexane). IR (KBr): 3056, 2926, 2858, 1715, 1573 cm^{-1}. ^{1}H-NMR (500 MHz, CDCl$_3$) δ: 2.35 (s, 3H, CH$_3$) 2.81 (s, 3H, CH$_3$), 6.56 (s, 1H), 7.73 (d, J = 9.2 Hz, 1H), 7.94 (d, J = 9.3 Hz, 1H), 9.31 (d, J = 9.2 Hz, 1H), 9.75 (d, J = 9.3 Hz, 1H). ^{13}C-NMR (125 MHz, CDCl$_3$) δ: 14.2, 25.0, 102.3, 109.3, 115.0, 118.4, 120.9, 125.1, 133.5, 133.6, 134.8, 145.1, 151.4, 152.5, 160.7, 161.5. LC–MS (ESI): m/z 264 [M − H]$^-$. HRMS (ESI): m/z [M + H]$^+$ calculated for $C_{16}H_{12}NO_3$: 266.0812, found: 266.0814.

3.3. Biological Experiments: In Vitro Assays

A 10 mM stock solution in DMSO was used. The compounds were diluted in 0.1% DMSO under sonification in an appropriate buffer in several dilutions, from which the determination of the IC$_{50}$ values was performed, at least in triplicate, and the standard deviation of absorbance was less than 10% of the mean. Statistical comparisons were made using the Student's *t*-test. A statistically significant difference was defined as $p < 0.05$. The compounds were dissolved in DMSO.

3.3.1. Inhibition of Linoleic Acid Peroxidation

The in vitro study was evaluated as reported previously by our group [40]. Ten microliters of the 16 mM sodium linoleate solution was added to the UV cuvette containing 0.93 mL of a 0.05 M phosphate buffer, pH 7.4, pre-thermostated at 37 °C. The oxidation reaction was initiated at 37 °C under air by the addition of 50 μL of a 40 mM AAPH solution, which was used as a free-radical initiator. Oxidation was carried out in the presence of the samples (10 μL from the stock solution of each compound) in the assay without antioxidants and monitored at 234 nm. Lipid oxidation was recorded in the presence of the same level of DMSO and served as a negative control. Trolox was used as the appropriate standard (positive control) (Table 4).

3.3.2. Soybean Lipoxygenase Inhibition Study

The in vitro study was evaluated as reported previously by our group [40]. The tested compounds were incubated in a tris buffer pH 9, at room temperature, with sodium linoleate (0.1 mM) and 0.2 mL of enzyme solution ($1/9 \times 10^{-4}$ *w/v* in saline, 1000 U/mL) for 5 min, and after that the inhibition was measured. EC 1.13.11.12 from soybean was used. The method was based on the conversion of sodium linoleate to 13-hydroperoxylinoleic

acid at 234 nm by the appearance of the conjugated diene. Nor-dihydroguaeretic acid NDGA (IC_{50} = 0.45 μM) was used as a standard (positive control). Different concentrations were used in order to determine the IC_{50} values. A blank determination was used first to serve as a negative control. The results are given in Table 4.

3.4. Docking Studies on Soybean Lipoxygenase

For the docking studies, soybean lipoxygenase-1 (PDB ID: 3PZW) was selected. The protein was prepared, including the removal of any water molecules cofactors or ions and adding all the missing residues following [72]. The hydrogen atoms and the AMBER99SBILDN charges were added and the iron atom charge was set to +2.0 with no restraint applied. OpenBabel was used for the generation of ligands' three-dimensional coordinates [73]. The ligands were minimized and ligand topologies were generated applying the MMFF94 force field [74], while for the ligand parameters ACPYPE (AnteChamber Python parser interface) was used [75], operating AnteChamber [76]. For the molecular dynamics simulation, the GROMACS 4.6 toolkit was applied [77], and for the energy minimization process, the AMBER99SB-ILDN force field was used [78]. Docking was performed with AutoDock Vina 1.1.2 by applying a 100, 70, 70 Å (in the x, y, z axes, respectively) grid box [79]. Interpretation of the results was performed using UCSF Chimera [80]. Docking calculations were carried out with an exhaustiveness value of 10 and maximum output of 20 docking modes.

4. Conclusions

New fused dipyranoquinolinones with amethyl substituent or diphenyl substituents in the pyridine moiety are prepared in excellent yields via the triple bond activation and *6-endo-dig* cyclization of propargyloxycoumarin derivatives using gold nanoparticles supported on TiO_2 in chlorobenzene under microwave irradiation. In the absence of gold nanoparticles, the methyl-substituted propargyloxypyridocoumarin derivatives resulted in fused furopyranoquinolinones through Claisen rearrangement and *5-exo-dig* cyclization. Among the biologically tested derivatives, **28a** presented potent inhibitory activity, whereas docking studies showed interactions with soybean lipoxygenase in an allosteric manner.

References

1. O'Kennedy, R.; Thornes, R.D. *Coumarins, Biology, Applications and Mode of Action*; Wiley: Chichester, UK, 1997; p. 1.
2. Fylaktakidou, K.; Hadjipavlou-Litina, D.; Litinas, K.; Nicolaides, D. Natural and synthetic coumarin derivatives with antiinflammatory/antioxidant activity. *Cur. Pharm. Des.* **2004**, *30*, 3813–3833. [CrossRef] [PubMed]
3. Kontogiorgis, C.; Detsi, A.; Hadjipavlou-Litina, D. Coumarin-based drugs: A patentreview (2008–present). *Expert Opin. Ther. Pat.* **2012**, *22*, 437–454. [CrossRef] [PubMed]
4. Vekariya, R.H.; Patel, H.D. Recent advances in the synthesis of coumarin derivatives *via* Knoevenagel condensation: A review. *Synth. Commun.* **2014**, *44*, 2756–2788. [CrossRef]

5. Stefanachi, A.; Leonetti, F.; Pisani, L.; Catto, M.; Carotti, A. Coumarin: A natural, privileged, and versatile scaffold for bioactive compounds. *Molecules* **2018**, *23*, 250. [CrossRef]

6. Hussain, M.I.; Syed, Q.A.; Khattak, M.N.K.; Hafez, B.; Reigosa, M.J.; El-Keblawy, A. Natural product coumarins: Biological and pharmacological perspectives. *Biologia* **2019**, *74*, 863–888. [CrossRef]

7. Tolba, M.S.; Abd ul-Malik, M.A.; Kamal El-Dean, A.M.; Geies, A.A.; Radwan, S.M.; Zaki, R.M.; Sayed, M.; Mohamed, S.K.; Abdel-Raheem, S.A.A. An overview on synthesis and reactions of coumarin based compounds. *Curr. Chem. Lett.* **2022**, *11*, 29–42. [CrossRef]

8. Heghes, S.C.; Vostinaru, O.; Mogosan, C.; Miere, D.; Iuga, C.A.; Filip, L. Safety Profile of Nutraceuticals Rich in Coumarins: An Update. *Front. Pharmacol.* **2022**, *13*, 803338. [CrossRef]

9. Miyata, R.; Shigeta, T.; Kumazawa, S.; Egi, M. Selective Syntheses of Coumarin and Benzofuran Derivatives Using Phenols and α-Methoxy-β-ketoesters. *SynOpen* **2023**, *7*, 8–16. [CrossRef]

10. Akkol, E.E.; Genç, Y.; Karpuz, B.; Sanchez, E.S.; Capasso, R. Coumarins and coumarin-related compounds in pharmacotherapy of cancer. *Cancers* **2020**, *12*, 1959. [CrossRef]

11. Wang, Y.T.; Yan, W.; Chen, Q.L.; Huang, W.Y.; Yang, Z.; Li, X.; Wang, X.H. Inhibition viral RNP and anti-inflammatory activity of coumarins against influenza virus. *Biomed. Pharm.* **2017**, *87*, 583–588. [CrossRef]

12. Al-Amiery, A.A.; Al-Majedy, Y.K.; Kadhum, A.A.; Mohamad, A.B. Novel Macromolecules Derived from Coumarin: Synthesis and Antioxidant Activity. *Sci. Rep.* **2015**, *5*, 11825. [CrossRef] [PubMed]

13. Hu, Y.-Q.; Xu, Z.; Zhang, S.; Wu, X.; Ding, J.-W.; Lv, L.Z.-S.; Feng, L.S. Recent developments of coumarin-containing derivatives and their anti-tubercular activity. *Eur. J. Med. Chem.* **2017**, *136*, 122–130. [CrossRef] [PubMed]

14. Ghobadi, E.; Ghanbarimasir, Z.; Emami, S. A review on the structures and biological activities of anti-Helicobacter pylori agents. *Eur. J. Med. Chem.* **2021**, *223*, 113669. [CrossRef]

15. Anand, P.; Singh, B.; Singh, N. A Review on Coumarins as Acetylcholinesterase Inhibitors for Alzheimer's Disease. *Bioorg. Med. Chem.* **2012**, *20*, 1175–1180. [CrossRef] [PubMed]

16. Zhang, R.R.; Liu, J.; Zhang, Y.; Hou, M.Q.; Zhang, M.Z.; Zhou, F.; Zhang, W.H. Microwave-assisted synthesis, and antifungal activity of novel coumarin derivatives: Pyrano [3,2-c] chromene-2,5-diones. *Eur. J. Med. Chem.* **2016**, *116*, 76–83. [CrossRef]

17. Venkataraman, S.; Meera, R.; Ramachandran, V.; Devi, P.; Aruna, A.; Parameswari, S.P.T.; Nagarajan, K. Antioxidant and anticoagulant activity of novel n-substituted-4- methyl-5,7-dihydroxyl coumarin and its ester derivatives. *Inter. J. Pharm. Rev. Res.* **2014**, *4*, 25–32.

18. Flores-Morales, V.; Villasana-Ruíz, A.P.; Garza-Veloz, I.; González-Delgado, S.; Martinez-Fierro, M.L. Therapeutic Effects of Coumarins with Different Substitution Patterns. *Molecules* **2023**, *28*, 2413. [CrossRef]

19. Rawat, A.; Reddy, A.V.B. Recent advances on anticancer activity of coumarin derivatives. *Eur. J. Med. Chem. Reports* **2022**, *5*, 100038. [CrossRef]

20. Markey, M.D.; Fu, Y.; Kelly, T.R. Synthesis of Santiagonamine. *Org. Lett.* **2007**, *9*, 3255–3257. [CrossRef]

21. Patra, P.; Patra, S. Mini Review on Pyrido[2,3-*c*]coumarins Backbone of Santiagonamine Antibiotics. *Heterocycles* **2023**, *106*, 241–269. [CrossRef]

22. Wang, X.-L.; Dou, M.; Luo, Q.; Cheng, L.-Z.; Yan, Y.-M.; Li, R.-T.; Cheng, Y.-X. Racemic alkaloids from the fungus *Ganoderma cochlear*. *Fitoterapia* **2017**, *116*, 93–98. [CrossRef] [PubMed]

23. Ahn, S.; Yoon, J.A.; Han, Y.T. Total Synthesis of the Natural Pyridocoumarins Goniothaline A and B. *Synthesis* **2019**, *51*, 552–556. [CrossRef]

24. Levrier, C.; Balastrier, M.; Beattle, K.D.; Carroll, A.R.; Martin, F.; Choomuenwai, V.; Davis, R.A. Pyridocoumarin, aristolactam and aporphine alkaloids from the Australian rainforest plant *Goniothalamus Australis*. *Phytochem.* **2013**, *86*, 121–126. [CrossRef]

25. Lu, Z.M.; Zhang, Q.J.; Chen, R.Y.; Yu, D.Q. Four new alkaloids from *Polyalthia nemoralis* (Annonaceae). *J. Asian Nat. Prod. Res.* **2008**, *10*, 656–664. [CrossRef]

26. Pang, M.; Lee, J.; Jeon, J.-H.; Song, I.-S.; Han, Y.T.; Choi, M.-K. Development of a Sensitive Analytical Method of Polynemoraline C Using LCMS/MS and Its Application to a Pharmacokinetic Study in Mice. *Mass Spectrom. Lett.* **2021**, *12*, 200–205. [CrossRef]

27. Gunatilaka, A.A.L.; Kingston, D.G.I.; Wijeratne, E.M.K.; Bandara, B.M.R.; Hofmann, G.A.; Johnson, R.K. Biological activity of some coumarins from Sri Lankan Rutaceae. *J. Nat. Prod.* **1994**, *57*, 518–520. [CrossRef]

28. Magiatis, P.; Melliou, E.; Skaltsounis, A.L.; Mitaku, S.; Leonce, S.; Renard, P.; Pierre, A.; Atassi, G. Synthesis and cytotoxic activity of pyranocoumarins of the seselin and xanthyletin series. *J. Nat. Prod.* **1994**, *57*, 518–520. [CrossRef]

29. Nivetha, R.; Bhuvaragavan, S.; Kumar, T.M.; Ramanathan, K.; Janarthanan, S. Inhibition of multiple SARS-CoV-2 proteins by an antiviral biomolecule, seselin from *Aegle marmelos* deciphered using molecular docking analysis. *J. Biomolec. Struct. Dynam.* **2021**, *40*, 11070–11081. [CrossRef]

30. Wittayapipath, K.; Laolit, S.; Yenjai, C.; Chio-Srichan, S.; Pakarasang, M.; Tavichakorntrakool, R.; Prariyachatigul, C. Analysis of xanthyletin and secondary metabolites from *Pseudomonas stutzeri* ST1302 and *Klebsiella pneumoniae* ST2501 against *Pythium insidiosum*. *BMC Microbiol.* **2019**, *19*, 78. [CrossRef]

31. Kang, S.Y.; Lee, K.Y.; Sung, S.H.; Park, M.J.; Kim, Y.C. Coumarins isolated from Angelica gigas inhibit acetylcholinesterase: Structure-activity relationships. *J. Nat. Prod.* **2001**, *64*, 683–685. [CrossRef]

32. de Moura, N.F.; Simionatto, E.; Porto, C.; Hoelzel, S.C.S.; Dessoy, E.C.S.; Zanatta, N.; Morel, A.F. Quinoline Alkaloids, Coumarins and Volatile Constituents of *Helietta longifoliata*. *Planta Med.* **2002**, *68*, 631–634. [CrossRef] [PubMed]

33. Morel, A.F.; Larghi, E.L. First total synthesis of (-)-(*R*)-geibalansin and (+)-(*S*)-geibalansin. *Tetrahedron Asymmetry* **2004**, *15*, 9–10. [CrossRef]

34. Sapkota, B.; Devkota, H.P.; Poudel, P. *Citrus maxima* (Brum.) Merr. (Rutaceae): Bioactive chemical substituents and pharmacological activities. *Hidawi Evid. -Based Complement. Altern. Med.* **2022**, *2022*, 8741669. [CrossRef] [PubMed]

35. Douka, M.D.; Litinas, K.E. An overview on the synthesis of pyridocoumarins with biological interest. *Molecules* **2022**, *27*, 7256. [CrossRef]

36. Patra, P.; Patra, S. 4-Aminocoumarin Derivatives as Multifaceted Building Blocks for the Development of Various Bioactive Fused Coumarin Heterocycles: A Brief Review. *Cur. Org. Chem.* **2022**, *26*, 1585–1614. [CrossRef]

37. Vlachou, E.-E.N.; Litinas, K.E. An Overview on Pyranocoumarins: Synthesis and Biological Activities. *Curr. Org. Chem.* **2019**, *23*, 2679–2721. [CrossRef]

38. Hsieh, W.-C.; Lin, C.-H.; Yang, Y.-J.; Yang, D.-Y. Multicomponent synthesis of pyrano[2,3-*c*] coumarins. *RSC Adv.* **2018**, *8*, 39162–39169. [CrossRef]

39. Vlachou, E.-E.N.; Fotopoulos, I.; Gabriel, C.; Pontiki, E.; Hadjipavlou-Litina, D.J.; Litinas, K.E. Synthesis and biological evaluation of fused dipyranoquinolinones as inhibitors of acetylcholinesterase with antioxidant properties. *Eur. J. Med. Chem. Reports* **2022**, *5*, 100063. [CrossRef]

40. Symeonidis, T.S.; Hadjipavlou-Litina, D.J.; Litinas, K.E. Synthesis Through Three-Component Reactions Catalyzed by FeCl₃ of Fused Pyridocoumarins as Inhibitors of Lipid Peroxidation. *J. Heterocycl. Chem.* **2014**, *51*, 642–647. [CrossRef]

41. Symeonidis, T.S.; Litinas, K.E. Synthesis of methyl substituted [5,6]- and [7,8]-fused pyridocoumarins via the iodine-catalyzed reaction of aminocoumarins with n-butyl vinyl ether. *Tetrahedron Lett.* **2013**, *54*, 6517–6519. [CrossRef]

42. Symeonidis, T.S.; Lykakis, I.N.; Litinas, K.E. Synthesis of quinolines and fused pyridocoumarins from N-propargylanilines or propargylaminocoumarins by catalysis with gold nanoparticles supported on TiO₂. *Tetrahedron* **2013**, *69*, 4612–4616. [CrossRef]

43. Symeonidis, T.S.; Kallitsakis, M.G.; Litinas, K.E. Synthesis of [5,6]-fused pyridocoumarins through aza-Claisen rearrangement of 6-propargylaminocoumarins. *Tetrahedron Lett.* **2011**, *52*, 5452–5455. [CrossRef]

44. Gautam, D.R.; Protopappas, J.; Fylaktakidou, K.C.; Litinas, K.E.; Nicolaides, D.N.; Tsoleridis, C.A. Unexpected one-pot synthesis of new polycyclic coumarin[4,3-c]pyridine derivatives via a tandem hetero-Diels-Alder and 1,3-dipolar cycloaddition reaction. *Tetrahedron Lett.* **2009**, *50*, 448–451. [CrossRef]

45. Galariniotou, E.; Fragos, V.; Makri, A.; Litinas, K.E.; Nicolaides, D.N. Synthesis of novel pyridocoumarins and benzo- fused 6-azacoumarins. *Tetrahedron* **2007**, *63*, 8298–8304. [CrossRef]

46. Vlachou, E.-E.N.; Balalas, T.D.; Hadjipavlou-Litina, D.J.; Litinas, K.E.; Douka, M.D. 2,9-Dimethyl-4H-oxazolo[5′,4′:4,5]pyrano[3,2-f]quinoline-4-one. *Molbank* **2023**, *2023*, M1591. [CrossRef]

47. Vlachou, E.-E.N.; Gabriel, C.; Litinas, K.E. One-pot Synthesis of Fused Dipyranocoumarins from Dihydroxycoumarins and Propargyl Chlorides under Microwave Irradiation. *J. Heterocyclic Chem.* **2019**, *56*, 99–107. [CrossRef]

48. Litinas, K.E.; Symeonidis, T.S. Convenient synthesis of fused pyrano[3,2-h]- and furo[3,2-h]benzo[f]coumarins from naphthalene-2,3-diols. *Tetrahedron* **2010**, *66*, 1289–1293. [CrossRef]

49. Tsoukka, M.; Litinas, K.E.; Nicolaides, D.N.; Hadjipavlou-Litina, D.J. Synthesis and biological evaluation of new benzo[f]furo[2,3-h]- and benzo[f]pyrano[2,3-h]coumarin derivatives. *J. Heterocyclic Chem.* **2007**, *44*, 529–534. [CrossRef]

50. Baldoumi, V.; Gautam, D.R.; Litinas, K.E.; Nicolaides, D.N. Convenient synthesis of linear pyrano[3,2-g]-. [2,3-g]- and angular pyrano[3,2-f]coumarins from 4-[(1,1-dimethyl-2-propynyl)oxy]phenol. *Tetrahedron* **2006**, *62*, 8016–8020. [CrossRef]

51. Nicolaides, D.N.; Gautam, D.R.; Litinas, K.E.; Hadjipavlou-Litina, D.J.; Fylaktakidou, K.C. Synthesis and evaluation of the antioxidant and anti-inflammatory activity of some benzo[l]khellactone derivatives and analogues. *Eur. J.Med. Chem.* **2004**, *39*, 323–332. [CrossRef]

52. Nicolaides, D.N.; Gautam, D.R.; Litinas, K.E.; Papamehael, T. Synthesis of some 3,4-dihydro-*2H*-benzo[f]pyrano[2,3-h]chromen-6-one derivatives. *J. Chem. Soc. Perkin Trans 1* **2002**, *33*, 1455–1460. [CrossRef]

53. Lin, S.T.; Yang, F.-M.; Yang, H.-J.; Huang, K.-F. Preparation of amino- and formylaminocoumarins by selective hydrogenation of nitrocoumarins. *J. Chem. Res.* **1995**, *27*, 372–373. [CrossRef]

54. Soares, A.M.S.; Costa, S.P.G.; Sameiro, M.; Gonçalves, T. Oxazole light triggered protecting groups: Synthesis and photolysis of fused heteroaromatic conjugates. *Tetrahedron* **2010**, *66*, 8189–8195. [CrossRef]

55. De, P. Efficient reduction of nitroarenes with SnCl₂ in ionic liquid. *Synlett* **2004**, *10*, 1835–1837. [CrossRef]

56. Uliassi, E.; Fiorani, G.; Krauth-Siegel, R.L.; Bergamini, C.; Fato, R.; Bianchini, G.; Menéndez, J.C.; Molina, M.T.; López-Montero, E.; Falchi, F.; et al. Crassiflorone derivatives that inhibit *Trypanosoma brucei* glyceraldehyde-3-phosphate dehydrogenase (*Tb*GAPDH) and *Trypanosoma cruzi* trypanothione reductase (*Tc*TR) and display trypanocidal activity. *Eur. J. Med. Chem.* **2017**, *141*, 138–148. [CrossRef]

57. Neetha, M.; Aneeja, T.; Afsina, C.M.A.; Anilkumar, G. An Overview of Ag-catalyzed Synthesis of Six-membered Heterocycles. *ChemCatChem* **2020**, *12*, 5330–5358. [CrossRef]

58. Efe, C.; Lykakis, I.N.; Stratakis, M. Gold nanoparticles supported on TiO₂ catalyse the cycloisomerisation/oxidative dimerisation of aryl propargyl ethers. *Chem. Commun.* **2011**, *47*, 803–805. [CrossRef]

59. Praveen, C.; Dupeux, A.; Michelet, V. Catalytic Gold Chemistry: From Simple Salts to Complexes for Regioselective C–H Bond Functionalization. *Chem. Eur. J.* **2021**, *27*, 10495–10532. [CrossRef] [PubMed]

60. Arcadi, A.; Ciogli, A.; Fabrizi, G.; Fochetti, A.; Franzini, R.; Ghirga, F.; Goggiamani, A.; Iazzetti, A. Synthesis of pyrano[2,3-*f*]chromen-2-ones *vs.* pyrano[3,2-*g*]chromen-2-ones through site controlled gold-catalyzed annulations. *Org. Biomol. Chem.* **2019**, *17*, 10065–10072. [CrossRef]

61. Lau, V.M.; Pfalzgraff, W.C.; Markland, T.E.; Kanan, M.W. Electrostatic Control of Regioselectivity in Au(I)- Catalyzed Hydroarylation. *J. Am. Chem. Soc.* **2017**, *139*, 4035–4041. [CrossRef]

62. Menon, R.S.; Findlay, A.D.; Bissember, A.C.; Banwell, M.G. The Au(I)-Catalyzed Intramolecular Hydroarylation of Terminal Alkynes Under Mild Conditions: Application to the Synthesis of 2*H*-Chromenes, Coumarins, Benzofurans, and Dihydroquinolines. *J. Org. Chem.* **2009**, *74*, 8901–8903. [CrossRef]

63. Ishii, H.; Ishikawa, T.; Takeda, S.; Ueki, S.; Suzuki, M. Cesium fluoride mediated Claisen rearrangement of aryl propargyl ether. Exclusive formation of 2-methylarylfuran and its availability as a masked salicylaldehyde. *Chem. Pharm. Bull.* **1992**, *40*, 1148–1153. [CrossRef]

64. Dorel, R.; Echavarren, A.M. Gold(I)-Catalyzed Activation of Alkynes for the Construction of Molecular Complexity. *Chem. Rev.* **2015**, *115*, 9028–9072. [CrossRef] [PubMed]

65. Furstner, A.; Davies, P.W. Catalytic Carbophilic Activation: Catalysis by Platinum and Gold π Acids. *Angew. Chem. Int. Ed.* **2007**, *46*, 3410–3449. [CrossRef] [PubMed]

66. Vlachou, E.-E.N.; Armatas, G.S.; Litinas, K.E. Synthesis of Fused Oxazolocoumarins from o-Hydroxynitrocoumarins and Benzyl Alcohol Under Gold Nanoparticles or FeCl3. *J. Heterocyclic Chem.* **2017**, *53*, 2447–2453. [CrossRef]

67. Ren, Q.; Kang, J.; Li, M.; Yuan, L.; Chen, R.; Wang, L. Regioselective Access to Structurally Diverse Coumarin Analogues through Iron-Catalysed Annulation Reactions. *Eur. J. Org. Chem.* **2017**, *2017*, 5566–5571. [CrossRef]

68. Kasthuri, J.K.; Singh, J.S.; Thripuram, V.D.; Gundabolu, U.R.; Ala, V.; Kolla, J.N.; Jayaprakash, V.; Ahsan, M.J.; Bollikolla, H.B. Synthesis, Characterization, Docking and Study of Inhibitory Action of Some Novel C-Alkylated Chalcones on 5-LOX Enzyme. *ChemistrySelect* **2017**, *2*, 8771–8778. [CrossRef]

69. Kostopoulou, I.; Tzani, A.; Polyzos, N.-I.; Karadendrou, M.A.; Kritsi, E.; Pontiki, E.; Liargkova, T.; Hadjipavlou-Litina, D.; Zoumpoulakis, P.; Detsi, A. Exploring the 2′-Hydroxy-Chalcone Framework for the Development of Dual Antioxidant and Soybean Lipoxygenase Inhibitory Agents. *Molecules* **2021**, *26*, 2777. [CrossRef]

70. Mavridis, E.; Bermperoglou, E.; Pontiki, E.; Hadjipavlou-Litina, D. 5-(4H)-Oxazolones and Their Benzamides as Potential Bioactive Small Molecules. *Molecules* **2020**, *25*, 3173. [CrossRef]

71. Mantzanidou, M.; Pontiki, E.; Hadjipavlou-Litina, D. Pyrazoles and Pyrazolines as Anti-Inflammatory Agents. *Molecules* **2021**, *26*, 3439. [CrossRef] [PubMed]

72. Fiser, A.; Šali, A.B.T.-M. Modeller: Generation and Refinement of Homology-Based Protein Structure Models. *Methods Enzymol.* **2003**, *374*, 461–491. [CrossRef]

73. O'Boyle, N.M.; Banck, M.; James, C.A.; Morley, C.; Vandermeersch, T.; Hutchison, G.R. Open Babel: An open chemical toolbox. *J. Cheminform.* **2011**, *3*, 33. Available online: http://www.jcheminf.com/content/3/1/33 (accessed on 7 October 2011). [CrossRef] [PubMed]

74. Halgren, T.A. Merck molecular force field. I. Basis, form, scope, parameterization, and performance of MMFF94. *J. Comput. Chem.* **1996**, *17*, 490–519. [CrossRef]

75. Sousa da Silva, A.W.; Vranken, W.F. ACPYPE—AnteChamber PYthon Parser interfacE. *BMC Res. Notes.* **2012**, *5*, 367. Available online: http://www.biomedcentral.com/1756-0500/5/367 (accessed on 23 July 2012). [CrossRef]

76. Wang, J.; Wang, W.; Kollman, P.A.; Case, D.A. Automatic atom type and bond type perception in molecular mechanical calculations. *J. Mol. Graph. Model.* **2006**, *25*, 247–260. [CrossRef] [PubMed]

77. Hess, B.; Kutzner, C.; van der Spoel, D.; Lindahl, E. GROMACS 4: Algorithms for Highly Efficient, Load-Balanced, and Scalable Molecular Simulation. *J. Chem. Theory Comput.* **2008**, *4*, 435–447. [CrossRef] [PubMed]

78. Lindorff-Larsen, K.; Piana, S.; Palmo, K.; Maragakis, P.; Klepeis, J.L.; Dror, R.O.; Shaw, D.E. Improved side-chain torsion potentials for the Amber ff99SB protein force field. *Proteins Struct. Funct. Bioinforma.* **2010**, *78*, 1950–1958. [CrossRef]

79. Trott, O.; Olson, A.J. AutoDock Vina: Improving the speed and accuracy of docking with a new scoring function, efficient optimization, and multithreading. *J. Comput. Chem.* **2010**, *31*, 455–461. [CrossRef]

80. Pettersen, E.F.; Goddard, T.D.; Huang, C.C.; Couch, G.S.; Greenblatt, D.M.; Meng, E.C.; Ferrin, T.E. UCSF Chimera—A visualization system for exploratory research and analysis. *J. Comput. Chem.* **2004**, *25*, 1605–1612. [CrossRef]